Engineering Bone-to-Bone Ligament with a Functional Enthesis Using a Modular Approach

By

ISMAEL BOUSSO

Thesis

Submitted in partial satisfaction of the requirements for the degree of

MASTER OF SCIENCE

in

Biomedical Engineering

in the

OFFICE OF GRADUATE STUDIES

of the

UNIVERSITY OF CALIFORNIA

DAVIS

Approved:

Prof. Keith Baar, Chair

Dr. Lucas Smith

Dr. Blaine Christiansen

Committee in Charge

2022

Acknowledgments

I would like to thank my advisor, Dr. Keith Baar, for all of his support, guidance, patience, and mentorship. I am grateful that you invited me into your group and for the invaluable experiences I have had along the way. You taught me how to be confident in my decisions and judgment. I would like to also thank my thesis committee members, Dr. Blaine Christiansen and Dr. Lucas Smith, for that time out of their busy schedules to review my thesis paper. I am grateful for all of my lab mates, who supported me through my journey. I would like to give thanks to Alek Avey, Nkechinyere Chidi-Ogbolu, Suraj Pathak, and Danielle Steffen for taking the time to teach me laboratory techniques and helping me get a grip on my project. I would like to thank the IMSD and UC Davis BMEGG faculty for their support in my endeavors.

Abstract

Anterior cruciate ligament (ACL) injuries are prevalent among athletes and the general public, resulting in socioeconomic stress, loss of performance, and decreased quality of life. Currently, surgical repair is the gold standard. However, these interventions are expensive and associated with limited improvement in quality of life due to the increased risk of post-traumatic osteoarthritis (PTOA). PTOA is due in part to the lack of recapitulation of the enthesis between the ligament and bone. Therefore, there is a need to develop alternative ways to improve ligament-to-bone grafting and promote the development of a functional enthesis. Tissue engineering techniques have emerged as one way to generate these tissues. Current tissue-engineered ligament grafts fail to mature completely, and usually fail at the ligament-bone interface. The purpose of this study was to use a two-step modular approach to promote enthesis formation and thereby improve the mechanical integrity of engineered ligaments. First, an enthesis construct was formed around individual brushite anchors. Second, a linear bone-to-bone ligament was formed using two enthesis anchors. Control constructs and constructs that controlled for the increased cell density (400k) were formed in parallel around two bare brushite anchors. Neither interface strength (MTL), ultimate tensile strength, collagen percentage, nor modulus was significantly different between the groups. Although, we observed a trend in interface strength, collagen content, and failure at the midsubstance with the modular constructs. Tissue infiltration at the anchor was observed, suggesting the initial formation of a tidemark. We also observed the presence of collagen X near the anchor. Although, it was less intense in the modular group.

Table of Contents

Chapter 1: Enthesis Formation, Healing, and Tissue Engineering Techniques

Introduction

The musculoskeletal system is composed of hierarchical structures that are all required to work in unison to facilitate movement and stabilize joints. Two of the less studied structures are tendons and ligaments, which help transmit forces between muscles and bone and bone and bone, respectively (Leong et al., 2020). Damage to these connective tissues accounts for 45% of musculoskeletal injuries in the United States (Butler et al., 2004), with a direct economic cost of over $40 billion.

Tendons and ligaments have several biomechanical and physiological adaptations that minimize injury. These include specialized structures at the tissue interfaces: the myotendinous junction connecting the muscle to the tendon and the enthesis connecting tendons and ligaments to bone (Lee-Barthel et al., 2018). Both interfaces contain zones that varying in mechanical properties in order to overcome the impedance mismatch between tissues with vastly different mechanical properties. In the enthesis, these regions include the tendon/ligament proper, unmineralized fibrocartilage, mineralized fibrocartilage, and bone (Benjamin et al., 2006). This complex and multiscale organization creates an interface that is often stronger than the associated bone, where failure results in avulsion fractures (where a small piece of bone breaks off) rather than injury to the interface itself. The intricacy of this interface presents significant clinical challenges, especially during tendon/ligament reconstruction surgery. In fact, the architectural structure and functionality of the enthesis is not recreated operatively. Current procedures, such as autografts and allografts, fail to reestablish the enthesis and predispose the repair site to re-injury (Moffat et al., 2008). Given the importance of the enthesis “organ” in the function of the musculoskeletal system and clinical challenges associated with recapitulation, there is a need for functional alternatives that will allow full integration of soft tissue-to-bone via regeneration of the enthesis.

Enthesis Structure and Function:

Entheses are transitional sites that attach tendons and ligaments to bone. The compositional gradient in tissue organization helps transmit contractile load from the more compliant tendon/ligament to the stiff bone. Work done by Michael Benjamin classifies entheses further into the distinct tissues, fibrous entheses and fibrocartilaginous entheses. Fibrous entheses, link stabilizing tendons and ligaments to bones using only a dense collagen zone, whereas fibrocartilaginous entheses have an additional transitional zone composed of fibrocartilage that transmits and dissipates the higher forces seen in load-bearing tissues more gradually (Benjamin et al., 1995; Benjamin & Ralphs, 1998). The importance of the transition between two dissimilar materials led to the proposition of the "enthesis organ" concept. The "enthesis organ" is defined by the complex integration of multiple tissues at the insertion site each serving to transmit and dissipate stress. These structures include a change in collagen orientation and cross-sectional area, a fat pad to provide lubrication and resistance to compression, the bursa, and trabecular bone(Benjamin & Mc Gonagle, 2001). The structure and pathology of the "enthesis organ" are extensively discussed elsewhere (Benjamin et al., 2000, 2004, 2006; Benjamin & Mcgonagle, 2009.; Benjamin & Mc Gonagle, 2001; Shaw et al., 2008) and will not be addressed in this thesis. Instead, this work will focus on the development and properties of the healthy fibrocartilaginous enthesis.

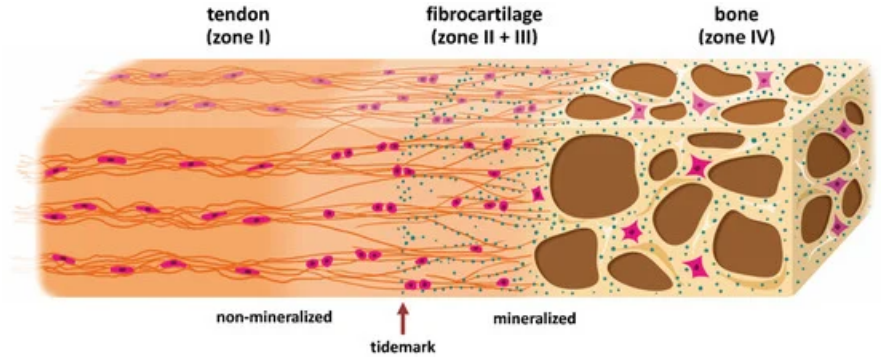

Smith, J., Petrovic, P., Rose, M., De Souz, C., Muller, L., Nowak, B., & Martinez, J. (2021). Placeholder Text: A Study. *The Journal of Citation Styles*, *3*. https://doi.org/10.10/X

Figure 1: Schematic representation of the fibrocartilaginous enthesis. The first zone is the tendon/ligament proper, consisting of elongated tenocytes embedded in a highly aligned collagen I matrix. The fibrocartilage region has the unmineralized zone (zone II) and mineralized zone (zone 3). Zone II, populated by ovoid fibro-chondrocytes, consists of type I, II, and III collagen. The tidemark marks the transition between the unmineralized, and mineralized fibrocartilage and is composed of mostly collagen X. In zone III, the fibrocartilage is mineralized by calcium phosphate and contains hypertrophic fibro-chondrocytes embedded in a type I and II collagen matrix. Zone III continuously transitions into the bone, which is highly mineralized and contains collagen I fibers, osteoclast, osteoblasts, and osteocytes. Note that the collagen alignment goes from highly aligned and unmineralized to less aligned and highly mineralized(Friese et al., 2020).

The fibrocartilaginous enthesis, as previously mentioned, involves a gradient transition from soft tissue to bone. A junction termed the tidemark differentiates the mineralized and unmineralized zones while the cement line marks the transition between fibrocartilage and bone. The process for early development of fibrocartilaginous enthesis requires mechanical loading and can be recapitulated during the formation of bony spurs in rat Achilles tendons(Benjamin et al., 2000).

Work from Benjamin and others suggests that tendon attaches to the original embryonic cartilaginous bone. Over time, the original cartilage in the rudimentary bone erodes during endochondral ossification and is replaced by entheseal fibrocartilage. Essentially, the bone grows into the tendon after fibrocartilage resorption resulting in the complex interdigitation of calcified fibrocartilage and bone within the enthesis (Benjamin et al., 2000). This interdigitation of collagenous fibers and a mix of cells allows for the modulation of mechanical forces. Each zone consists of different characteristics that play an important role in the function of the organ. The tendon/ligament region consists of mechanosensitive fibroblasts, termed tenocytes and ligamentacytes, that are embedded in a specialized extracellular matrix comprised of aligned type I collagen (Banos et al., 2008; Rossetti et al., 2017; Takimoto et al., 2015). As the tendon or ligament moves towards to bone, the cross-sectional area expands and the orientation of the

collagen changes to align perpendicular to the bone at the insertion site. As the area and orientation of collagen change, the aspect ratio within the tendon/ligament decreases beyond the 4:1 ratio necessary for tensional loading, progressively increasing compression on the embedded cells. This shift in load is sensed by the cells producing a change in cellular structure: rounded fibro-chondrocytes within the unmineralized and hypertrophic chondrocytes within the mineralized zone. The different cells also produce different collagen matrices (shifting from predominantly type I to type II collagen) and the fibrocartilaginous matrix flares and interlocks with the bone across a wide surface area to increase the stability of the interface between the soft tissue and bone (Benjamin et al., 2006; Rossetti et al., 2017). Anchorage over a wide surface area reduces stress concentrations and provides protection to the interface by preventing fibers from bending acutely at tissue lines (Benjamin et al., 2006; Benjamin & Ralphs, 1998; Hems & Tillmann, 2000; Shaw & Benjamin, 2007).

The Enthesis ECM

The extracellular matrix in the enthesis plays a pivotal role in transmitting tensile forces, which is critical due to the bone side of the superstructure exhibiting significantly higher modulus than the tendon/ligament. The fibrocartilaginous transitional zone at the enthesis is rich in type II collagen, proteoglycans, fibromodulin, and tenascin (Rossetti et al., 2017). Glycosaminoglycans (GaGs) and proteoglycans accumulate within the matrix as collagen fiber diameter decreases (Puetzer et al., 2021). In tendons and ligaments, the proteoglycans decorin, biglycan, tenomodulin, and fibromodulin, regulate collagen fibril length, spacing, diameter, and therefore are essential to tissue mechanics. Within the fibrocartilaginous zones, the proteoglycans shift to larger structures like aggrecan that hold more water and provide greater compressive strength. Collagen proteins are also expressed spatially with type I collagen, expressed by osteoblasts and tenocytes/ligamentocytes, aligning matrix within the tendon/ligament, and mineralized in

bone along the line of tension. Type II and III collagen, characteristic of chondrocytes, localize to the unmineralized zone with other proteins such as aggrecan. The calcified zone predominantly contains types II and X collagen, expressed by hypertrophic chondrocytes (Benjamin et al., 1995; Rossetti et al., 2017; Schwartz et al., 2015). The collagen fiber alignment at the enthesis is optimized to take force from all directions (Golman et al., 2021). The hypothesized role of type X collagen at the tidemark is to prevent the spread of calcification and maintain the separation between mineralized and unmineralized tissues. The bone region consists of osteoblasts, osteoclasts, and osteocytes surrounded by a type I collagen matrix (Tsukamoto et al., 2006). Together, these compositional gradients of matrix and mineral vary the elastic and viscous behavior of the tendon/ligament and bone, minimizing impedance mismatch and the resulting stress/strain concentrations.

Biological Factors Necessary of Entheseal Development and Formation

Several biological factors have been shown to drive the formation of the enthesis, such as loading (Baker et al., 2011), tissue-specific transcription factors, and hormonal cues (i.e. bone morphogenic proteins (BMPs), transforming growth factor (TGF), and the hedgehog signaling pathway (Blitz et al., 2009; Breidenbach et al., 2013a; Lee-Barthel et al., 2018; Roberts et al., 2019).

Transcriptional Cues

Fibrocartilaginous entheses develop from a distinct pool of cells that express the transcription factors Scleraxis (Scx) and Sry-related HMG box 9 (Sox-9), which are necessary for tenogenesis and chondrogenesis, respectively(Asou et al., 2002). These progenitor cells are recruited during the formation of the enthesis primordia to form bone eminences, the sites of tendon attachment (Blitz et al., 2013). Id et al., (2020) recently examined the localization of

$Scx^+/Sox9^+$ cells in neonatal, young, and old mice to elucidate the involvement of the cells in the postnatal formation of the fibrocartilaginous enthesis. The researchers observed wide distribution of $Scx^+/Sox9^+$ cells from the insertion site of the supraspinatus tendon prior to the formation of the entheseal fibrocartilage layer (figure 2). Over time, the cells localized around the developing fibrocartilage surface of the bone and tendon, leading to a mature fibrocartilaginous entheses. Additionally, Studies done with Scx knockout mice showed impaired enthesis attachment strength, loss of the cellular and mechanical gradient, decreased bone ridge formation, and reduced loading during entheseal development, suggesting that Scx is necessary for interface formation(Killian & Thomopoulos.,2016).

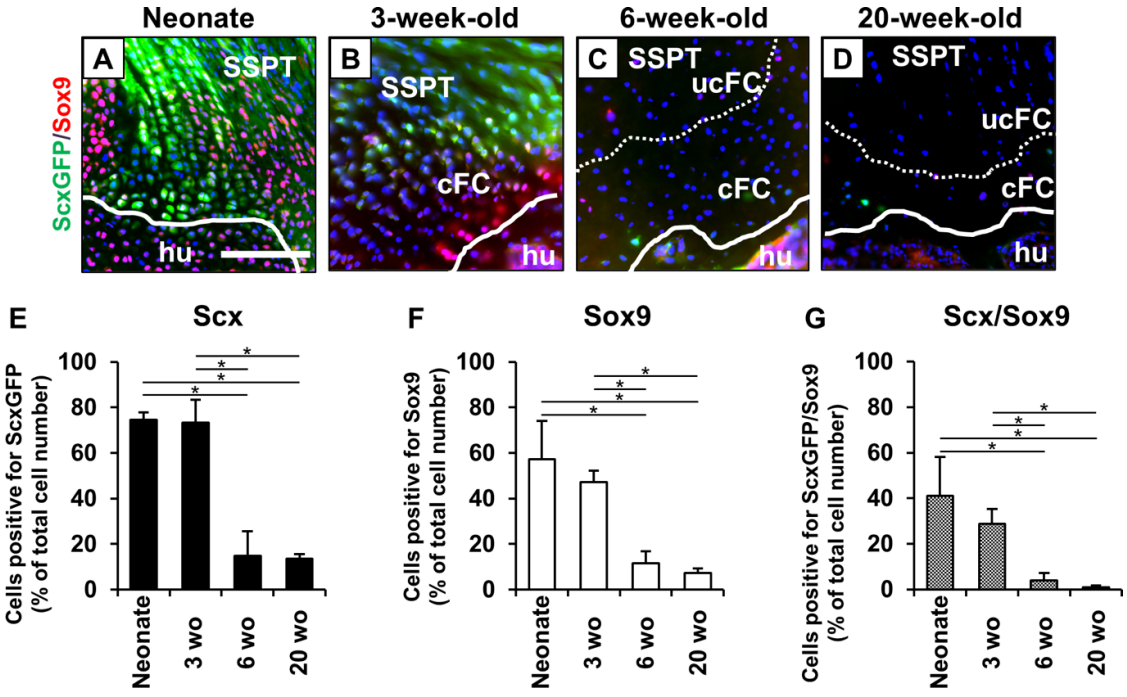

Id, K. I., Tokunaga Id, T., Shukunami, C., Takimoto, A., Yoshimoto, Y., Yonemitsu, R., Karasugi, T., Mizuta, H., Hiraki, Y., & Miyamoto, T. (2020). *Role of Scx + /Sox9 + cells as potential progenitor cells for postnatal supraspinatus enthesis formation and healing after injury in mice*. https://doi.org/10.1371/journal.pone.0242286

Figure 2: Scx/Sox9 cells present in the postnatal formation of the fibrocartilaginous enthesis and decrease over a time. Immunostaining of $Sox9^+$ (red) and Scx^+ (red) cells in the supraspinatus tendon (SSPT), humerus (hu), mineralized fibrocartilage (cFC) demonstrates a decrease of these cell populations during development. At the 6-week time point, unmineralized fibrocartilage (ucFC) gets pushed closer to the calcified region (A-D). E-F represents

the number of cells positive for SoxGFP, Sox9, and ScxGFP/Sox9 as a percent of total cell number, respectively (Id et al., 2020).

Hormonal Cues

The expression of Scx is controlled by both load and hormonal factors. TGFβ signaling is necessary for the specification and maintenance of the chondroprogenitors that make up the primordial bone (Blitz et al., 2013). In contrast, the BMP4 pathway differentiates $Scx^{+}/Sox9^{+}$ cells into the chondrocytes that form the initial attachment between tendons and bone during development (Blitz et al., 2013). Transcriptomic analysis of early mouse limb development shows that TGFβ is the predominant driver of Scx-expression through the activation of SMAD2/3 signaling (Pryce et al., 2009). However, ablation of BMP4 and TGFβ from Scx-expressing cells results in poor enthesis formation and complete loss of Scx-expression in developing tendons (Blitz et al., 2009; Pryce et al., 2009), suggesting that both endocrine and autocrine mechanisms are needed for interface formation. The mechanism by which TGFβ regulates enthesis formation is still controversial. Clayton and colleagues suggest that TGFβ regulates the expression of Scx via ERK1/2, depending on cell type, microenvironment, and development stage (Clayton et al., 2020). By contrast, Pryce, et al., (2009) found Scx upregulation in mouse limb progenitors after inhibition of the ERK1/2 signaling pathway. Together, these data suggest that coordinated temporal and spatial expression of these molecular signals regulates the formation of the enthesis primordia during development.

Fibrocartilaginous formation and maturation of the enthesis are also regulated postnatally by a population of hedgehog-responsive (Hh) cells (Breidenbach et al., 2013b; Schwartz et al., 2015). Hedgehog-responsive cells regulate chondrocyte differentiation and homeostasis and drive the mineral gradient within the enthesis (Schwartz et al., 2015). As described above, enthesis progenitors are distributed from the tendon midsubstance to the

primary cartilage population within the bone. These cells synthesize a collagen template that anchors to the eminence and proteoglycans that provide compressive strength as the cells mature into unmineralized fibrocartilage. During mineralization, the mature cells express alkaline phosphatase and type X collagen in response to Hh signaling through upregulation of the cell surface protein Smoothened (SMO) (Breidenbach et al., 2013b; Dyment, Breidenbach et al., 2015; Schwartz et al., 2015). Specifically, Indian hedgehog (Ihh) expressed by pre-hypertrophic chondrocytes binds to the membrane protein Patched (Ptch), activating SMO, initiating a signaling cascade that includes proteins such as GLI-Kruppel family member 1, 2, and 3 (Gli1/2/3) (Bangs & Anderson, n.d.; Dyment, Breidenbach, et al., 2015). Gli1 then amplifies the transcriptional response of hedgehog signaling. Cells expressing Gli1 eventually replace sox9 progenitors and populate the fibrocartilage region between the tendon and bone throughout postnatal development (Felsenthal et al., 2018; Schwartz et al., 2015). This suggests that Gli+ cells play an integral role in the maturation and mineralization of the fibrocartilaginous insertion. Knockout of Hh and SMO reduce the expression of extracellular matrix proteins such as tenascin C, type 2 collagen, and large proteoglycans like aggrecan. There is also evidence of aberrant tidemark formation, mineralization, and chondrocyte proliferation and differentiation (Breidenbach et al., 2013a; Schwartz et al., 2015). The activation of Hh signaling also establishes a negative feedback loop with parathyroid hormone-related proteins (PTHrP), providing precise spatial and temporal control of molecules critical for chondrocyte proliferation and endochondral ossification. PTHrP promotes chondrocyte proliferation while inhibiting maturation during cartilaginous osteogenesis (Han et al., 2016). This is achieved through the downregulation of BMP signaling by RunX2 (Han et al., 2016), a transcription factor integral to osteoblast differentiation. Elevated expression of PTHrP at the entheses is essential to formation of mineralized interfaces during development (Provot & Schipani, 2005; Wang et al., 2014). Consistent with this finding, the Ablation of PTHrP in Scx^{+} cells lead to phenotypic abnormalities during enthesis formation (Wang et al., 2014).

Biomechanical Cues

The strength of the tendon is a function of type I collagen fibers laid out in parallel arrays to transmit force in a uniform direction (Benjamin et al., 1995; Felsenthal et al., 2018). Collagen in the tendon organizes to form a hierarchical structure consisting of microfibril, fibril, fiber, and fascicles bundled together to form the whole tendon/ligament (figure 3). This orientation of collagen plays a role in the anisotropic viscoelastic characteristics of the tendon/ligament, optimizing directional energy absorption and force transfer. The mechanical behavior of tendons and ligaments can change dramatically due to age, injury, or disease. Relationships between load and degeneration have been reported (LaCroix et al., 2013; Magnusson et al., 2010; Thomopoulos et al., 2011), although the role of mechanical stress in tissue homeostasis is not fully understood. The transduction of mechanical cues is pivotal in developing, healing, and regenerating the tendon and enthesis. Recently, the gap junction protein connexin-43 (Cx43) was proposed as a key mediator of mechanoresponsiveness and the formation of a functional interface (Shen et al., 2020). Interestingly, Cx43 is thought to be required for the Hh signaling. Shen et al. (2020) showed that mice lacking Cx43 in tendon and the enthesis exhibited limited ability to perform treadmill running. This was not due to changes in mouse size, strength, or physical activity; rather, it was caused by the inability of the tendon and enthesis to respond to loading. The authors suggest that Cx43 is not required to maintain the tendon microarchitecture due to the similarity in tendon CSA and tenocyte organization between the WT and KO mice. Instead, the mechanical properties of the enthesis from knockout mice had decreased maximum tensile strength, stiffness, and young's modulus. Additionally, the knockout group had a higher rupture rate than the wild type.

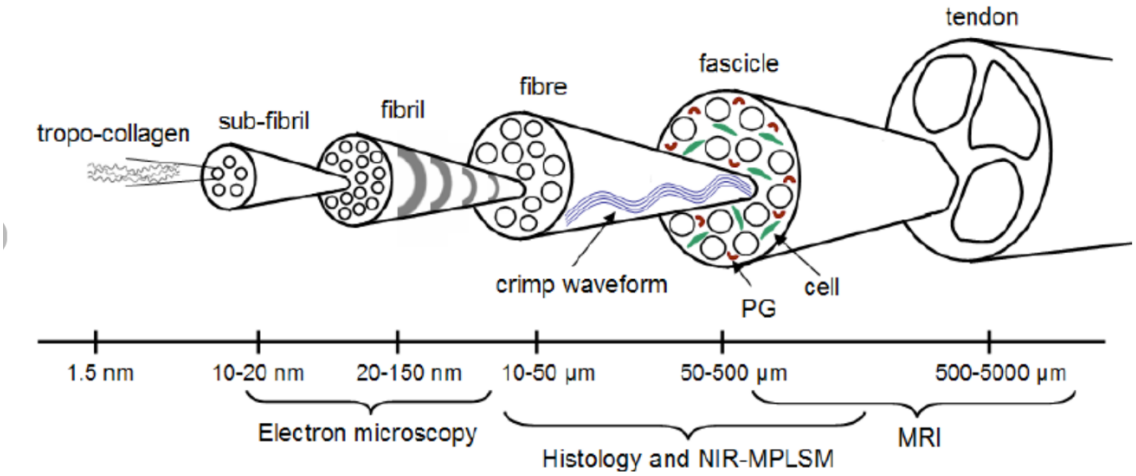

Harvey, A. K., Thompson, M. S., Cochlin, L. E., Raju, P. A., Cui, Z., Cornell, H. R., Hulley, P. A., & Brady, S. M. (2009). Functional Imaging of Tendon. *Annals of the BMVA*, *2009*(8), 1–11.

Figure 3: Hierarchical structure of tendons/ligaments. The largest structure is the tendon/ligament made up of multiple fascicles. The fascicles contain fibrils which play pivotal roles in tendon viscoelastic mechanics. The crimp provides the nonlinear relationship of the stress-strain curve (toe region). The basic structure in the complex is tropo-collagen (Harvey et al., 2009)

.

The enthesis requires a combination of compressive and tensile stress to maintain function and mineralization. The requirement for load may be a direct effect of the load on cell fate or may change the production of paracrine factors. TGFβ signaling is increased in response to mechanical load through upregulation of matrix metalloproteases (MMPs), or by upregulation of the early growth response 1 (Egr1) transcription factor (Gaut et al., 2016; T. Maeda et al., 2011). The effects of TGFβ depends seems to depend on loading conditions. Excessive loading conditions excessive TGFβ can lead to tenocytic apoptosis and damage to the ECM (E. Maeda et al., 2009; T. Maeda et al., 2011). Load-induced increases in collagen I synthesis in tendon are correlated with increases in TGFβ levels; however, whether this is a causal relationship has yet to be determined (Cillo et al., 2000; Heinemeier et al., 2003). Since Egr1 has been shown to upregulate TGFβ, it is possibly one of the mechanosensory proteins in developing tendon-to-bone tissues. Reducing the load across engineered ligaments results in the downregulation of Egr1 and tendon genes. Transfection with Egr1 is enough to preserve the expression of Scx,

type I collagen, and tenomodulin even without the mechanical stimulus (Gaut et al., 2016). Further, in injured rat Achilles tendons subjected to mechanical loading Egr1 is one of five genes uploaded within 15 minutes, suggesting a role for Egr1 during tendon healing (Eliasson et al., 2013).

Mechanistic experiments using tendon constructs *in vitro* show that other pathways can be activated by loading. These pathways include Akt/mTORC1, ERK1/2, and focal adhesion kinase (FAK) signaling (Paxton et al., 2010, 2012). Importantly, the activation of ERK1/2 is required to increases collagen expression in response to load (PMID: 14985070). Further, when an exercise protocol is designed to maximize ERK1/2 phosphorylation, the result is a doubling of collagen content in the engineered tissue (Paxton et al., 2012). Given the discussion above, it is important to note that ERK1/2 activation lies upstream of Egr1 expression (Eliasson et al., 2013a; Herchenhan et al., 2020). Therefore, there is a direct molecular pathway from the activation of ERK1/2 to the increase in Egr1 and the subsequent activation of collagen synthesis in response to load. However, whether there are interactions between transcription factors (Egr1 and Scx) and/or signaling pathways (TGFβ and Hh) in response to mechanical stimuli remains to be determined.

Muscle-dependent Loading for Postnatal Enthesis Formation

The formation of the tendon-to-bone attachment is initially independent of muscle loading. During postnatal development, tendon entheses require a combination of compressive and tensile forces from skeletal muscle contraction for maintenance and mineralization of the structure. Avey & Baar, (2021) have extensively reviewed the potential crosstalk mechanisms between muscles and tendons. However, signaling between bone and tendon is equally important. In the absence of muscle loading, induced by chemical denervation of neonatal mice,

the tendon and enthesis do not form properly, with the tendon showing disorganized collagen fiber alignment and the enthesis losing fibrocartilage gene expression (Thomopoulos et al., 2007). Thomopoulos and colleagues also demonstrated that paralyzed mouse shoulders exhibited a slower fibrocartilage mineralization rate and larger porosity at the enthesis insertion (Thomopoulos et al., 2007). Overall, postnatal development of the enthesis is delayed by decreased mechanical loading. As discussed above, during normal enthesis development chondrocytes become hypertrophic and mineralize to form the transitional zone. These chondrocytes, within the lacunae of the ECM, are arranged in a columnar pattern perpendicular to the subchondral plate (Benjamin et al., 1995; Benjamin & Ralphs, 1998; Thomopoulos et al., 2007). Muscle unloading decreases the viability of chondrocytes and alters their hypertrophic phenotype resulting in changes in morphological characteristics (Järvinen et al., 2003; Thomopoulos et al., 2007). Although tendons mainly undergo uniaxial loading, dynamic compressive loading is linked to the development of fibrocartilage in bovine models, especially where tendon fibers insert into the bone at an oblique angle (Benjamin & Ralphs, 1998). Aggrecan synthesis is decreased during the unloading of adult bovine disks, and this is attenuated by cyclic compressive loads. Fibrocartilage at the enthesis provides a low permeability environment, reducing stress concentrations between a fluid tendon and solid bone (Benjamin & Ralphs, 1998). ECM proteins such as MMPs and proteoglycans are synthesized during compressive loading conditions in developing tendons(Evanko & Vogel, 1993; E. Maeda et al., 2009). Additionally, compression enhances type II collagen, aggrecan, and GaG expression, all of which are required to maintain the tendon-to-bone microenvironment (Li et al.,2010). Brown & Puetzer (2021) studied the effect of compressive mechanical boundary conditions and the addition of beta-tricalcium phosphate (βTCP), a known osteoconductive agent, on the development of zonal ligament-to-bone entheses. The authors found that compressive boundary clamps guide ligament fibroblasts to produce three unique zones of collagen organization and GAGs, type II, and type X collagen levels. Essentially, by six weeks

of culture the constructs showed ECM organization and composition similar to that of immature bovine entheses. Reducing mechanical stress by unloading leads to reduced tendon elastic properties (Almeida-Silveira et al., 2000). Functionally, this reduces force transmission between the muscle and bone. Unloading also alters collagen within the tissue, remodeling to reduce the size and organization of the fibrils. Interestingly, decreasing muscle activity by hindlimb unloading or paralysis yield different results on the enthesis. During hindlimb unloading, loads are still transmitted through the tendon as a result of muscle contraction, whereas following paralysis zero force transmission is seen in the tissue. Overall, loading through tendons/ligaments are required for the development, remodeling, and maintenance of the enthesis environment.

Effects of Cyclic Loading on Enthesis: Bone Interface

The morphology of the enthesis seems to depend on the type, frequency, and direction of load. A number of studies have looked at bone formation as a function of the type of loading. Intermittent cyclic mechanical tension (ICMT) with a 10% tension strain at 0.5Hz resulted in calcification of end-plate chondrocytes (Xu et al., 2012). ICMT reduced the expression of cartilage-like specific ECM markers such as type II collagen, aggrecan, and sox-9. Instead, the cells began to express type I and X collagen, osteocalcin, and osteopontin, which are markers of endochondral ossification and bone formation. Tsukamoto et al. (2006) similarly observed ligament ossification in rat spines with cyclic tensile loading. Accumulating repetitive tensile stress induced the proliferation of round cells, formation of cartilaginous tissue, and woven bone near the insertion of the spinal ligaments. The authors suggest it could have been due to unequal distribution of forces and different sensitivity in each ligamentous element in spinal ligaments. Although, the cause could be due accumulation of stress and microdamage of the ligament. Subsequently, the infiltration of other cell populations or change to a compressive load

sharing environment, priming the tissue for mineralization. The stiffness and strength of bone and mineralized fibrocartilage are dependent on the mineralization of the organic matrix. Over-mineralization makes these regions brittle and less fatigue resistant. Thus, over-mineralizing the insertion site can lead to diseases such as enthesopathy and osteoarthritis. Saito et al. (2021) observed that the absence of mechanical stress eradicated the transitional fibrocartilage and creased the collagen fibrils in the enthesis, which decreased the strength and structural integrity of the tissue. Fibrocartilage hierarchical structure was maintained under 1mm (0.5hz) elongation cyclic loading, while 2mm elongation (0.5hz) caused cellular apoptosis, collagen fragmentation, and calcification. Therefore, the magnitude, frequency, and duration of load appear to dictate enthesis homeostasis.

Enthesis Healing

Attaching two dissimilar materials, such as tendon and bone, is a clinical challenge. In the uninjured state, the tendon/ligament has a modulus of ~200GPa, while the bone has a modulus of ~20GPa. The natural gradation at the interface facilitates the effective transfer of tensile loads while reducing stress concentrations. Current repair techniques have not been effective in promoting enthesis regeneration. Carmel Vinestock et al., (2021.) recently found a novel healing mechanism for neonatal entheses that might provide clues for regenerating this organ. Following injury to the neonatal enthesis, the local ECM resident cells formed a hypocellular and avascular scar rather than healing through inflammation and angiogenesis. The authors showed that mice who received a neonatal injury to their enthesis were able to return to normal motility within two months suggesting a mechanically competent tissue was formed. However, the authors completed neither mechanical tests nor histological analysis of the regenerated interface. Studies observing the effects of mechanical load on soft tissue to bone healing demonstrate that application of cyclical load improves the unit's healing (Bedi et

al., 2010; Dagher et al., 2009). Although the injured ACL tissues in these models underwent healing, the functional gradience of the enthesis was not recreated. What transpired was the resolution of acute inflammation that resulted in more effective healing. This finding suggests that reducing macrophages drastically decreases fibrosis formation, thus effectively reestablishing collagen fiber continuity for healing. Several in-vitro studies using co-culture suggest that environmental factors could affect interface regeneration (Calejo et al., 2018; Jiang et al., 2005; Mosher et al., 2015). When Jiang et al. (2005) co-cultured chondrocytes and osteoblasts they noted no change in cell proliferation but did find differential gene expression between the cells was maintained. Chondrocytes produced GAGs and type II collagen, while osteoblasts produced type I collagen and demonstrated high ALP activity. The interesting result was that co-culture suppressed mineralization and delayed osteoblast-mediated suppression. The interaction between the two cell types appears to regulate metabolic activity, matrix production, and cell phenotype. The same authors also tested osteogenic medium on a co-culture of hASCs and hTDC, they observed increased enthesis marker, tenascin, and aggrecan. They also found increased expression of Runx2, a marker of differentiation of chondrocytes to hypertrophic chondrocytes. Although these co-culture systems resulted in phenotypic changes and increased expression of enthesis-related makers, fibrocartilage was not formed.

Interestingly, age-related cellular and microstructural changes also influence enthesis healing. Long et al. (2021) found that well-aligned collagen fibers in rotator cuffs entheses become highly disorganized with age. Additionally, the contact between tendon and bone decreases due to the diminishing nonmineralized fibrocartilage and cellularity. As expected, proliferation and wound healing decrease with age. Therefore, when thinking about enthesis healing, we must consider different factors such as the surrounding soft tissue structures, modulation of key regulators, and the mechanism of repair processes to effectively find a solution for soft tissue to bone healing. If the enthesis cannot be recapitulated surgically, a

mismatch of material properties between tendon and bone will causes stress concentrations, diminished mechanical properties, and increased likelihood of re-injury.

Tissue Engineering for Interface Regeneration

Given the clinical challenges for the regeneration of soft tissue-to-bone interfaces, tissue engineering techniques are being applied to forming entheses in vitro and in vivo. The development of a mix therapy using scaffold-based therapies with co-cultures has been explored in enthesis regeneration. Fibrocartilage-like structures with Type I, II, and III collagen were created using a triphasic scaffold seeded with human tendon fibroblasts and osteoblasts on opposite ends of the scaffold (Spalazzi et al., 2006, 2008). The result was a tissue that looked like an enthesis. Specifically, a continuous collagen matrix formed across the three scaffold phases, a bone-like matrix formed on one end and a collagen rich matrix formed on the other. These 3-layered scaffolds are produced using PLGA microspheres to mimic soft tissue, fibrocartilaginous region, and bone. These scaffolds allow for controlled manipulation of matrix stiffness and provide the complexity in the structure required for mimicking multi-tissue formation. One can exercise precise spatial control over mineral distribution over the scaffold using polymers and ceramics. The limitation is that the tensile properties of these scaffolds have not been tested, and whether having an enthesis without an attached ligament would be useful for surgical repairs has yet to be demonstrated.

Engineering 3-D bone-to-bone ligament proper tissues with osteoconductive bone cements (brushite) can result in a graded tissue interface (Paxton et al., 2012). Paxton et al. utilized mechanical boundary conditions to guide cells to produce aligned fibrils. Specifically, by placing two brushite cement anchors at either end of a 35mm plate and forming a fibrin-based sinew around the anchors allows the cells within the organoid to create the uniaxial tension

necessary to align the cells along the line of force and for the cells to produce an aligned matrix. Near the anchors, the matrix becomes less aligned and raman spectrophotometric images show calcium crystals forming a gradient near the anchors, suggesting that the cells reorganize the brushite to make a pseudoenthesis.

Work from the same lab demonstrated that treating the anchor with BMP-4 increased enthesis failure load. The effect of BMP-4 was mediated by localized changes in expression with enthesis-related genes increasing with increasing doses of BMP-4. McCorry et al. (2017) created a similar model for engineered meniscus enthesis by seeding fibro-chondrocytes in mechanically bound decellularized bone plugs. This resulted in a uniaxially directed collagen matrix transitioning from a soft tissue to bone structure. These studies are some of the few that consider the implantation aspect of engineered tissues. Other groups fail to consider that engineered soft tissues lacking a bony interface must be attached directly to the hard tissue, which may make the structure prone to failure.

Recently, nanofiber scaffolds have been explored to re-engineer the tendon and bone unit. These scaffolds are highly manipulable, matching the native enthesis in collagen alignment, surface area to volume ratio, permeability, and porosity (Nowlin et al., 2018). Electrospinning allows precise control of collagen fiber alignment, fiber diameter, and scaffold pore sizes. MSCs can interact with their microenvironment and can differentiate into various lineages depending on the stiffness of scaffolds, fiber size, fiber diameter, and porosity of the matrix. In the study, the topography of the scaffold with intercellular interactions promoted enthesis formation (Nowlin et al., 2018). In summary, to remedy the issue of interface regeneration, researchers must establish ways to create both chemical and mechanical gradients within tissue-engineered scaffolds. In addition, these scaffolds must be engineered with an implantation strategy in mind.

Conclusion

The enthesis is a highly specialized organ that nature has engineered as a solution to decrease the mismatch in mechanical properties between two dissimilar materials. The material and mineral gradient within the enthesis gives it the capacity to withstand tensile, compressive and shear stresses and slowly transition from a compliant tissue to a tissue two orders of magnitude stiffer. Biochemical and biomechanical signals play an integral role in the development and maintenance of the enthesis. The material's mechanical response is heterogenous depending on the angle and direction of load, allowing the tissue to dissipate forces and prevent strain concentrations. Mechanical stimuli regulate enthesis homeostasis, composition, and strength. To properly treat and repair enthesis failure, it is pivotal to understand the phenotypic and chemical changes in the enthesis during different loading and developmental stages.

Chapter 2: Engineering 3D Bone-to-Bone Ligament with a Functional Enthesis Using a Modular Approach

Introduction

The enthesis is a functionally graded transitional tissue that connects tendons/ligaments to the bone, consisting of four distinct but continuous regions (Leong et al., 2020; Lee-Barthel et al., 2018). These four regions, tendon/ligament, unmineralized fibrocartilage, mineralized fibrocartilage, and bone, are spatially variable in their extracellular matrix (ECM) composition, structural organization, mechanical properties, and cellular phenotype (Lee-Barthel et al., 2018). During a connective tissue injury such as an anterior cruciate ligament rupture, the enthesis's function can be impaired, leading to an increased risk of re-injury.

Functionally, the enthesis acts to transmit tensile forces from tendon/ligaments to bone while minimizing stress concentrations at the transition (Martinez-Lemus et al., 2018). This is, impart, mediated by the presence of glycosaminoglycans in the fibrocartilage, providing a swelling pressure that resists compressive effects (Li et al.,2010) . Collagen fibrils also transition from highly aligned to random as the soft tissue wraps around and interdigitates with the bone (Benjamin et al., 2006; Rossetti et al., 2017).

Surgical interventions that maintain the enthesis such as a bone-patellar tendon-bone autografts result in significant donor site morbidity and predispose the patellar tendon to rupture. Thus, for the donor tissue preferred for grafting has shifted to hamstring autografts even though this graft lacks an enthesis (Lee-Barthel et al., 2018; Mosher et al., 2015; Spalazzi et al., 2006). Although autografts have high success rates due to limited immune rejection and disease transmission, the increased donor-site morbidity, absence of a functional enthesis can promote poor healing and lead to post-traumatic osteoarthritis (Gardinier et al., 2014; Salmon et al.,

2006). By contrast, the other graft option, allografts are ripe with issues including the increased risk of disease transmission and loss of strength during decellularization, resulting in a 4-fold greater re-rupture rate (Gorschewsky et al., 2005).

To improve soft tissue-to-bone repair, advanced therapies are needed to recapitulate the naturally complex enthesis. Tissue engineering has emerged as a promising alternative for mitigating the adverse effects of soft tissue to bone repair (Lee-Barthel et al., 2018). Tissue-engineered grafts can potentially recapitulate the enthesis and better incorporate with bone, thus, lowering the rate of re-failure. We previously used mechanical boundary conditions to guide cells to form 3D bone-to-bone ligaments by encapsulating human ACL fibroblast cells in a fibrin gel between two brushite cement anchors. This method promotes rapid tissue formation and using cells from the patient would reduce the possibility of rejection, disease transmission, and donor site morbidity associated with autografts (Lee-Barthel et al., 2018). However, despite the incorporation of many different methods for engineering ligaments, the fabrication of high tensile strength tendons/ligaments that can reach strength values comparable to native human tissues has been a challenge (Dyment, Breidenbach et al., 2015; Paxton et al., 2010; Thomopoulos et al., 2011). Furthermore, there are limitations in forming a functional enthesis, including structural and mechanical maturity of the tissue required for clinical use.

With this background, I hypothesized that adding extra tissue around the brushite cement anchors using a two-step modular approach would better recapitulate the enthesis and improve the mechanical integrity of engineered ligaments. To test the hypothesis, I utilized a two-step modular approach in which enthesis tissue was formed around individual brushite anchors for five days. Two of these enthesis anchors were then used in the formation of the engineered ligament. Control constructs (with bare anchors) and constructs that controlled for

the increased cell density (400k) in the enthesis ligaments were used to determine whether the extra tissue improved enthesis formation and interface strength.

Materials and Methods

All materials were obtained from Sigma (St. Louis, MO) unless indicated below.

Fabrication of Brushite Anchors

Brushite cement anchors were fabricated as previously described (Paxton et al., 2010). Briefly, Minutemen inspect pins were inserted in custom-made silicone anchor molds (tear drop shaped) before brushite cement paste was placed into the mold. To make the brushite cement, ß-tricalcium phosphate (solid-phase) was combined with orthophosphoric acid and 100mM citric acid (liquid-phase) at a 1:1 ratio (1g/ml) and mixed on ice for 20 seconds. Brushite cement-filled molds were spun at 3700rpm for 15s and then left to set a room temperature to set overnight. Individual anchors were removed from the mold the following day and placed in 25ml of non-sterile PBS on a rotator for 15min to clean off loose debris. Anchors were then left to dry and stored at room temperature until usage.

Formation of Enthesis Constructs

Enthesis constructs were fabricated as previously described (Lee-Barthel.,2018) with some modifications. Briefly, Individual brushite cement anchors were pinned onto sylgard-coated 24-well plates, and plates with anchors were sterilized in 70% ethanol for an hour. DMEM growth media supplemented with 10% fetal bovine serum and 1% penicillin/streptomycin combined with 1.74 units of thrombin solution containing $7.5x10^4$ hACL cells was added to each well and agitated to cover the surface. 1.72mg of fibrinogen (Lot: F4883-5g) was added dropwise, resulting in 300µl of fibrin gel that was left to gelatinize at 37ºC for 15min. The fibrin gel constructs were fed every two days with 500µL fully supplemented DMEM growth media

containing 200μM ascorbic acid (AA), 50μM L-proline, and 5ng/mL TGF-ß1. Constructs were cultured for five days before transferring to 35-mm sylgard-coated plates to form engineered 3D bone-to-bone ligaments.

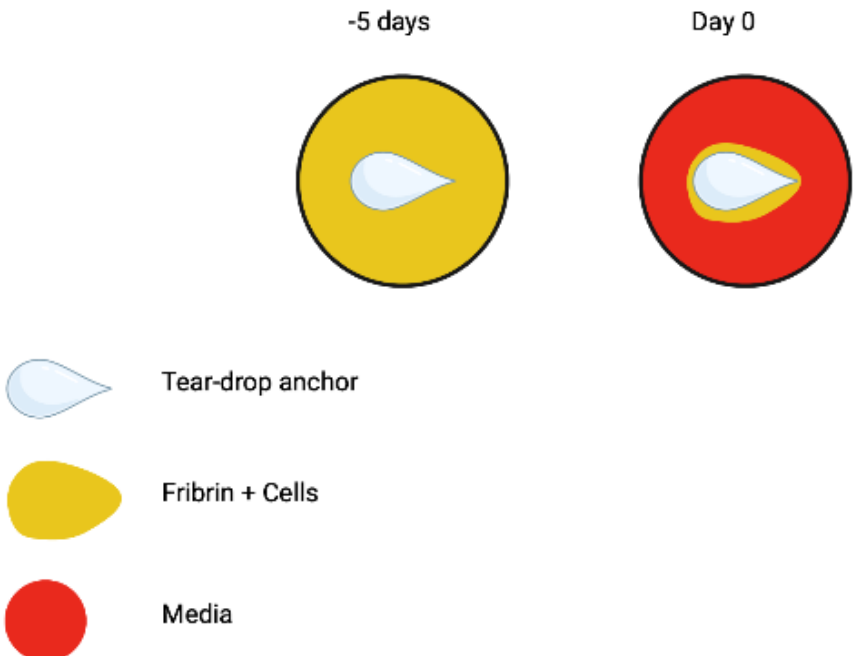

Figure 4: Rendering of Enthesis construct formation for modular group. Enthesis constructs were formed by embedding 7.5x10^4 hACL fibroblasts into a fibrin gel—the gel contracts around the tear-drop-shaped brushite anchor pinned onto sylgard-coated 24-well plates. Enthesis constructs were cultured for five days before transferring to 35-mm sylgard-coated plates to form linear modular group ligaments.

Formation of Ligament

Tissue-engineered ligament constructs were engineered as previously described with some modifications (Lee-Barthel et al., 2018; Paxton et al., 2010, 2012). Briefly, two brushite cement anchors were pinned 12mm apart in a sylgard-coated 35 mm dish. For individual constructs, human ACL fibroblasts were suspended in growth media containing 5.8 units of thrombin, 20μg of aprotinin, and 2μg of 6-aminohexanoic acid. 714μL of this cell/thrombin

solution was dispersed onto each plate. The enthesis and control (control) constructs contained $2.5x10^5$ cells. Since each enthesis construct contained $7.5x10^4$ cells ($1.5 x10^5$ for a pair), a second control group containing $4.0x10^5$ cells was added to control for the cell number. Modular constructs were engineered using two enthesis constructs. After addition of 286µL of a 20mg/ml solution of fibrinogen the graft was left to polymerize at 37ºC with 5% CO_2 for 15min. After formation, constructs were fed 2mL of growth media supplemented with 5ng/ml TGF-ß1, 200µM AA, and 50µM L-proline every two days for 14 days.

Figure 5: Image of the linear 3D engineered ligament. All groups (control, 400k, and modular exhibit similar phenotypes after 14 days in culture. Differentiating the modular group is an extra tissue layer around the anchors. Unmodified brushite anchors (control and 400k) were pinned into sylgard-coated 35-mm dishes. Linear ligament was formed for the control and modular groups by seeding $2.5x10^5$ cells + fibrin gel in the 35-mm dish. 400k group, serving as a cell control for the modular group, was seeded with $4x10^5$.

Uniaxial Tensile Testing

Tensile testing was performed as described previously with modifications (Larkin et al., 2006; Lee-Barthel et al., 2018; Paxton et al., 2010). Briefly, before testing, each construct's dimensions were determined via a digital caliper, and the ligaments were loaded into 3D-printed

custom grips connected to an Instron 6800. The samples were immersed into a phosphate-buffered saline bath at 37ºC and subjected to 10 preconditioning cycles (0.1N at 0.30mm/s). The tensile test used a constant elongation rate of 0.30mm/s until failure, and the resultant force was assessed. All samples used for analysis demonstrated a linear slope in the stress-strain (young's modulus) curve and a clear failure (ultimate tensile) strength (UTS). The interface strength of each construct was assessed using the maximal tensile load (MTL) since samples classically fail at the interface between the tissue and brushite anchor.

Hydroxyproline (Collagen Content)

The collagen content of the ligament constructs was determined via hydroxyproline analysis as previously described with some modifications (Paxton et al., 2010; Woessner, 1961). Briefly, after mechanical testing ligament constructs were removed from the cement anchors and dried at 120ºC for 30 minutes. Samples were then weighed and hydrolyzed in 200µL of 6 N HCl at 120ºC for 2 hours. The liquid was removed by heating samples to 100°C for 1.5 hours, resulting in a pellet that was resuspended in 200µL of hydroxyproline buffer. Samples were then diluted 1:10 for a final volume of 200µL in hydroxyproline buffer. 150µL of chloramine T solution was added to each sample and standard (range from 0-20mg/ml), mixed, and incubated at room temperature for 20 minutes. 6mL of 1-propanol and 2.6mL of perchloric acid were added to 1.5g 4(dimethylamino)benzaldehyde to form aldehyde-perchloric acid. 150µL of aldehyde-perchloric acid was added to each sample, vortexed, and incubated at 60ºC for 15 minutes. After incubation, samples were left to cool for 10 minutes and read at 500nm on an Epoch Microplate Spectrophotometer (BioTek Instruments Limited, Winooski, VT). Hydroxyproline was converted to collagen using a factor of 13.7%, as previously reported. Collagen percentage was calculated by dividing collagen content by the mass of the samples.

Cryosection, Histology, and immunohistochemistry

On day 14, constructs were washed twice in PBS, fixed in 4% paraformaldehyde for 48 hours, and decalcified overnight in 10% formic acid. Post decalcification, constructs were embedded in O.C.T compound (Sakura Finetek USA Inc., Torrance, CA) and frozen in liquid nitrogen-chilled isopentane.14µm sections were collected via a Leica CM3050S cryostat (Leica Biosystems Inc., Buffalo Grove, IL) and processed for histological examination. Hematoxylin and eosin (H&E) were used to visualize general cellular and morphological structures. Sirius red staining was used to assess collagen orientation. Co-incubation of collagen I + collagen X was used to determine enthesis formation. Samples were imaged using a Leica DMi8 inverted microscope. For comparative analysis, exposure length remained fixed for all samples. For all stains, overlapping images were stitched together such that the entire structutre could be analyzed at once.

Sirius red staining

Sirius red staining was conducted as previously described (Trensz et al., 2010). Briefly, Sections were circled with a PAP pen, rinsed with dH_2O 3 times for 5 minutes, and air dried for 15 minutes. Next, samples were stained in picrosirius red solution for 1 hour and washed with two changes of acidified water for 1 minute each. A dehydration cycle (3x1minute) was conducted with 100% ethanol. Finally, samples were cleared in citrisolv for 3 minutes, mounted with permount (toluene), and sealed with sealant.

Collagen I and X Immunohistochemistry

Frozen sections were dried at room temperature for 30 minutes and circled with a PAP pen. Next, the samples were blocked in 1%milk, 1%BSA, and 0.01% triton in PBS for 60 minutes. After blocking, samples were co-incubated with Collagen I (anti-goat IgG 1:200) and

collagen X anti-mouse IgG 1:200) primary antibodies for 1.5 hours at room temperature. Antibody X-AC9 (collagen X) was purchased from the Developmental Studies Hybridoma Bank (Iowa City, Iowa). Post incubation, samples were washed three times for 3 minutes in PBS. Secondary antibodies (goat-anti-mouse Alexa Fluor 488 for collagen X, donkey anti-goat Alexa Fluor 647 for collagen I) were incubated for 1 hour at room temperature. Finally, 1:2000 Hoechst 3342 trihydrochloride trihydrate was used to counterstain nuclei, and then samples were mounted with ProLong Gold and imaged via Leica DMi8 inverted microscope using HC PL FLUOTAR 5x/0.10 PH1 objective (Leica Microsystems, Wetzlar, Germany). For comparative analysis, exposure length remained fixed for all samples. For all stains, overlapping images were stitched together such that the entire muscle could be analyzed.

Statistical analysis

All data are presented as means ± standard deviation (SD) except for fail-spot frequency data. Each trial (T1-4) is representative of the different experiments across multiple donors. Experimental outcomes were normalized for donor variation except for fail-spot frequency. Statistical analysis was performed using GraphPad Prism 9 (GraphPad Software, Inc., La Jolla, CA). All data points (and hence sample size) were shown within each bar, excluding frequency data. One-way ANOVA was used to determine the presence of statistical significance between experimental conditions with Tukey's posthoc analysis when appropriate. Statistical analyses and the type I error were maintained at $\alpha < 0.05$ for all comparisons.

Results

Morphology

There was no difference in the cross-sectional area (CSA) between groups (SF 1). The average CSA across each group range between 0.4-0.6mm^2. After normalizing all groups to

control, there was not a significant difference in CSA. On average, there was not a significant difference in mass between groups (SF 4), suggesting that the addition of extra cells in the constructs does not change the morphology of the engineered ligament.

Effects of enthesis constructs on mechanical properties of engineered ligaments

To assess whether adding extra tissue around the brushite anchors would increase the structural integrity of 3D bone-to-bone engineered ligaments, enthesis constructs were engineered for 5 days before creating linear ligaments. There was no statistical difference in interface strength, measured by the MTL. When comparing biological replicates, each technical replicate for a given experiment was normalized to the average value of the control group. Despite there being no significant difference, there was a trend toward an increase in MTL and UTS with modular constructs (Figures 6 and 7). The modular construct had a 35% and 1% difference in interface strength compared to the control and 400k, respectively. The UTS of the modular construct was 47% and 27% higher than the control and 400k groups, respectively. There was no difference in modulus between the control, 400k, and modular group (figure 8).

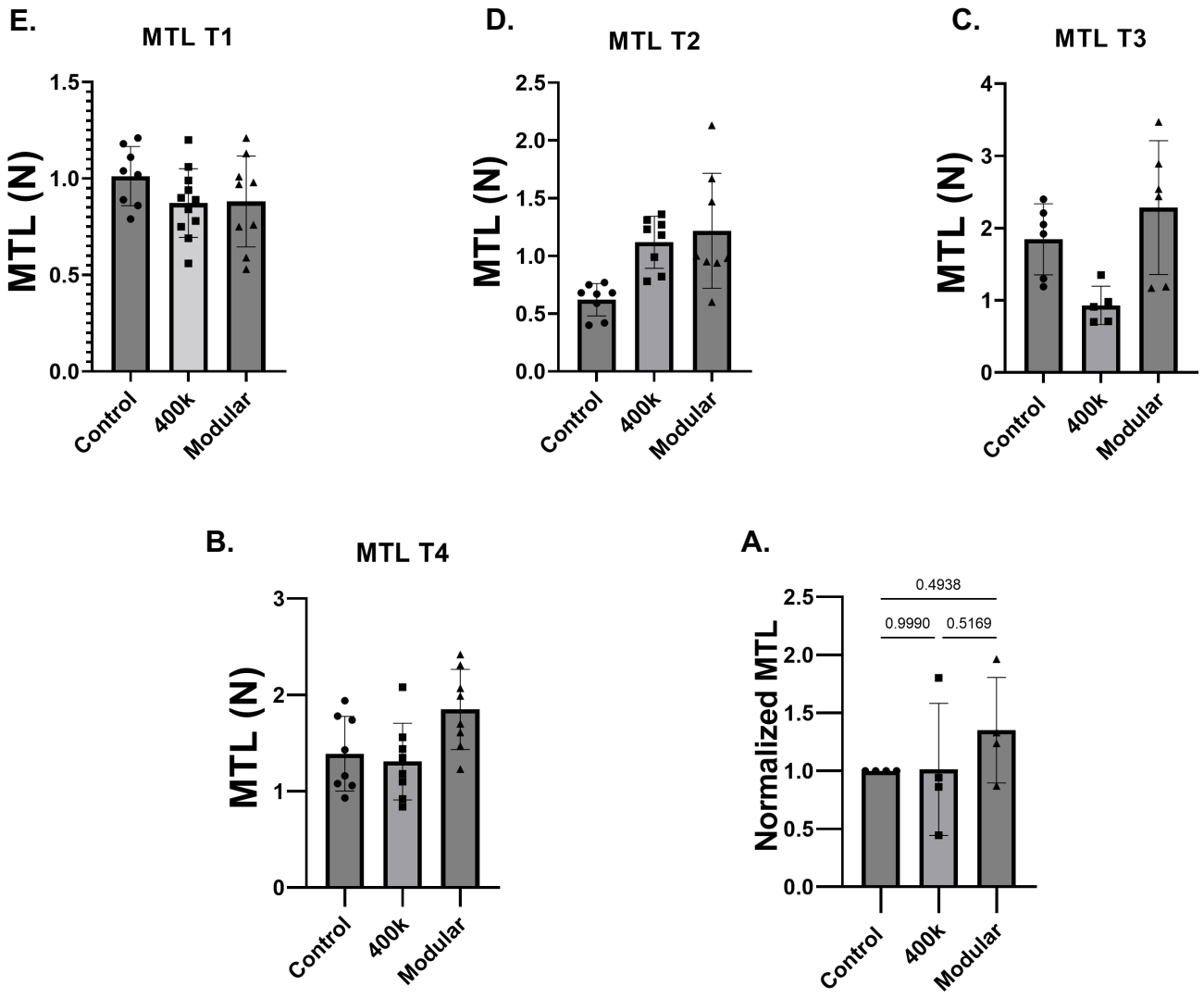

Figure 6. No statistical difference in maximal tensile load. Interface strength of control, 400k (cell-control), and modular groups across different biological replicates (A-D) and (E) a composite where the average of the technical replicates of each biological replicate are plotted together. T1 is representative of donor 1. T2 is the 2nd donor. T3 and T4 are the representation of hACL fibroblast cells from donor 3. A P-value of < 0.05 is to be considered statistically significant.

.

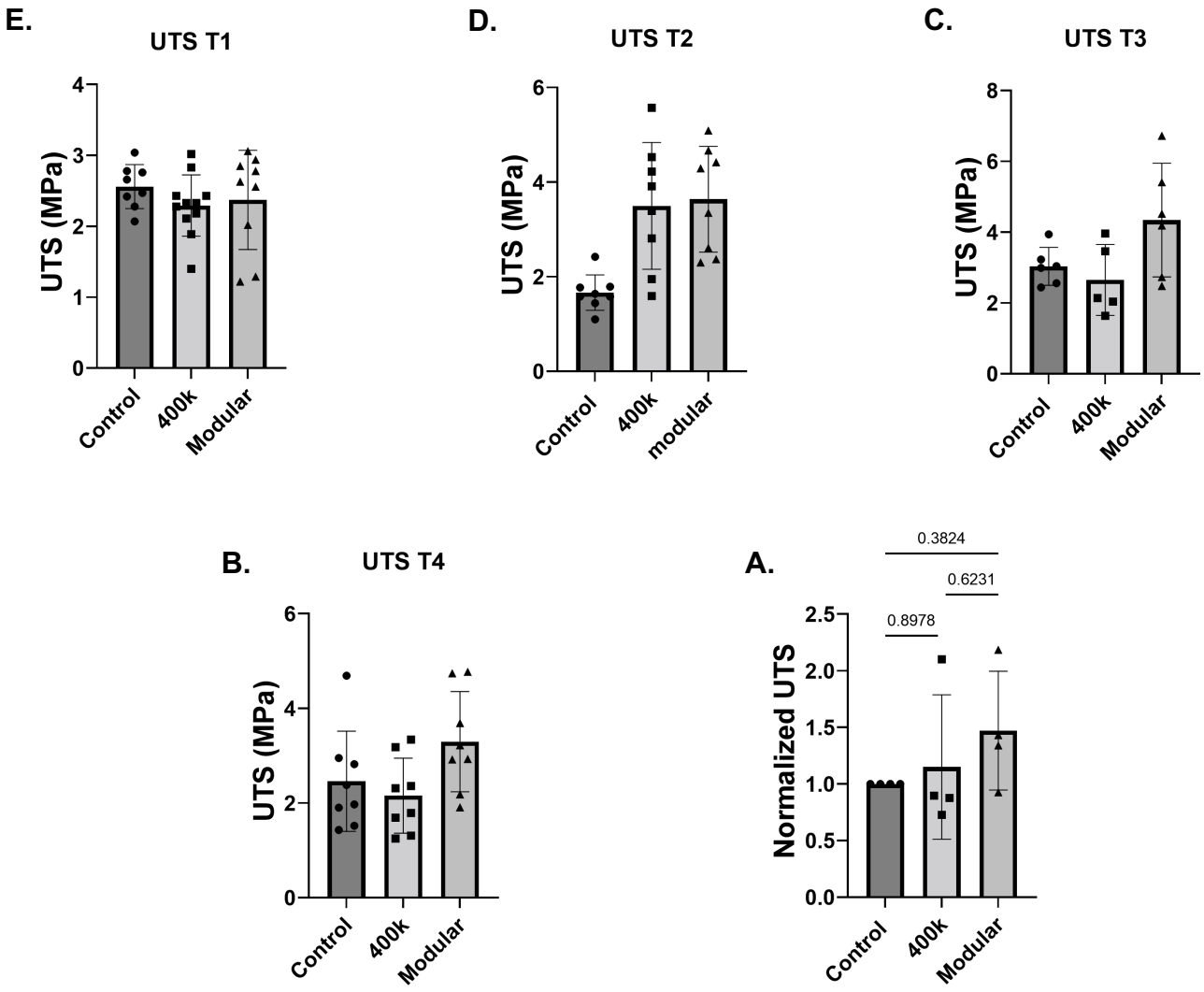

Figure 7. No statistical difference in ultimate tensile strength. UTS of control, 400k (cell-control), and modular groups across different biological replicates (A-D) and (E) a composite where the average of the technical replicates of each biological replicate are plotted together. T1 is representative of donor 1. T2 is the 2nd donor. T3 and T4 are the representation of hACL fibroblast cells from donor 3. A P-value of < 0.05 is to be considered statistically significant.

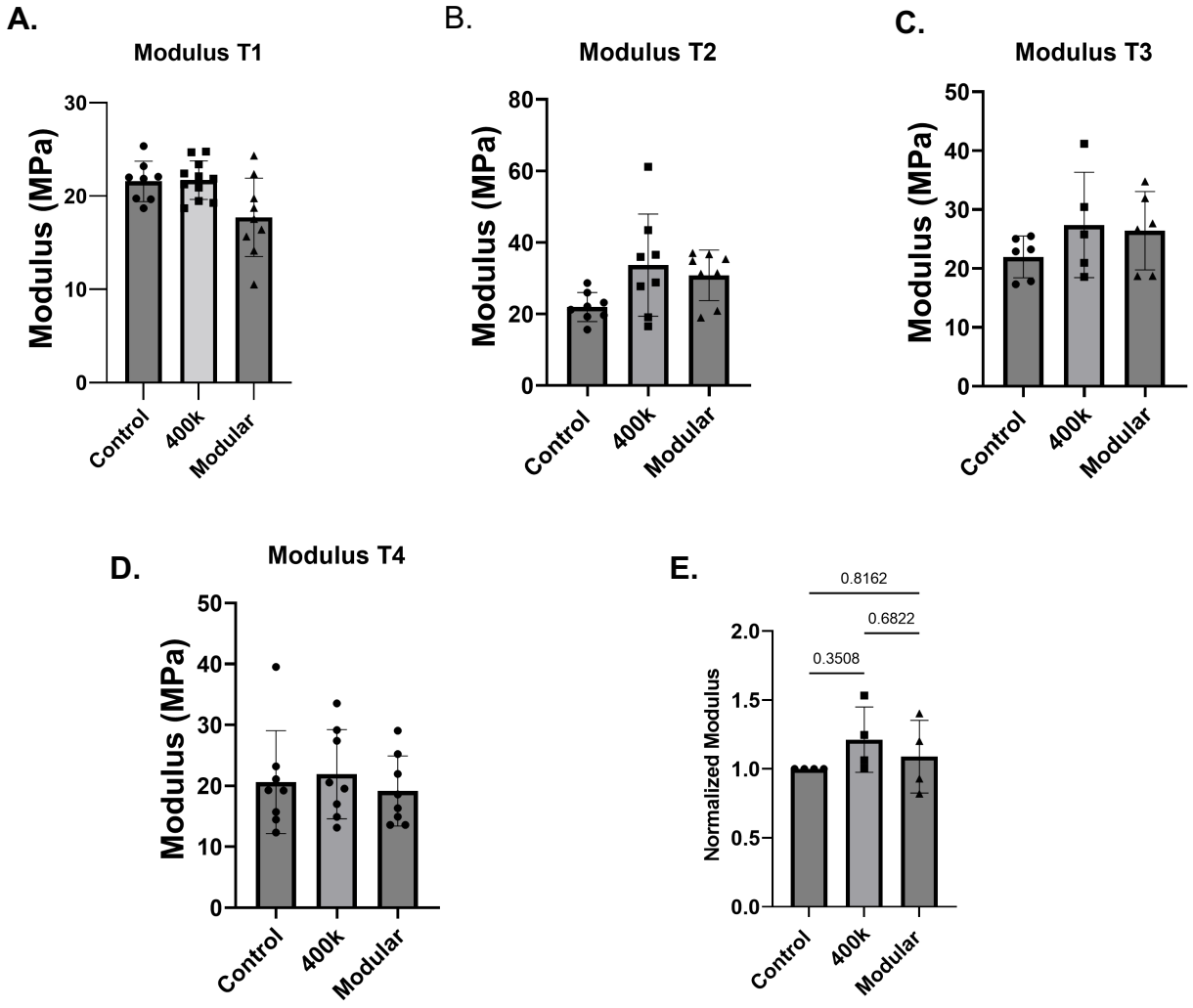

Figure 9. No statistical difference in modulus. Young's modulus of control, 400k (cell-control), and modular groups across different biological replicates (A-D) and (E) a composite where the average of the technical replicates of each biological replicate are plotted together. T1 is representative of donor 1. T2 is the 2nd donor. T3 and T4 are the representation of hACL fibroblast cells from donor 3. A P-value of < 0.05 is to be considered statistically significant.

Modular constructs decrease the frequency of anchor failure

We observed a higher failure frequency at the midsection for the modular ligaments compared to the control and 400k groups (Figure 10 and SF 5). Whereas 93.3% of the control and 87.5% of the 400K constructs failed at the anchor, only 58% of the modular constructs failed at the anchor and many of these contained significant amounts of brushite in the soft tissue.

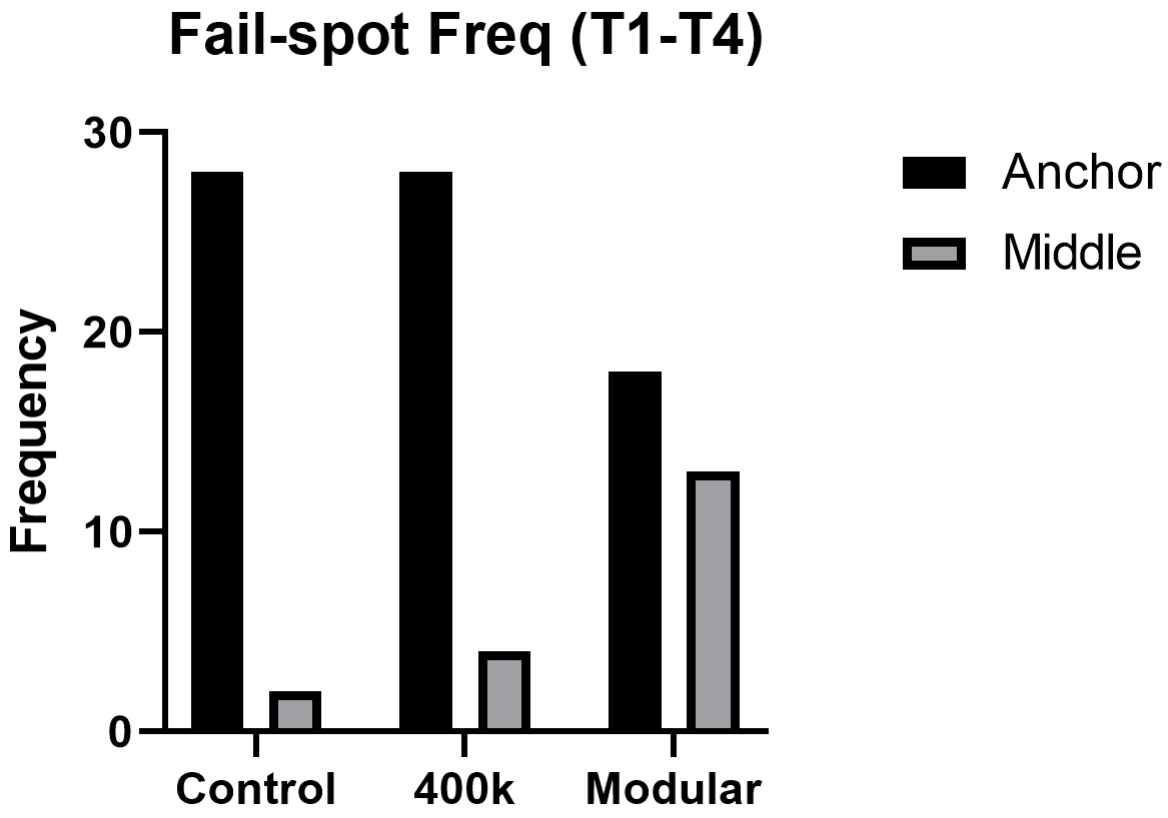

Figure 10. Enthesis constructs increases middle failure. Fail-spot frequency (middle, anchor) of control, cell control (400k), and modular group. Graph is representative of the sum of the technical replicates of each biological replicate are plotted together (T1-T4).

Collagen content and percentage in engineered constructs

Total collagen content significantly increased compared to control (49% compared to control). Although normalized collagen content was not different between the modular and 400k groups, modular constructs had an average of 31.8% higher collagen content (SF 2). In contrast, there was no difference in collagen percentage of dry mass, which appeared to plateau at ~ 26% after 14 days of incubation (SF 3). This was due to a slight increase in collagen mass (SF 4).

Enthesis constructs exhibit greater tissue penetration into brushite anchor

In the picrosirius redlight microscopy, collagen fibers appeared dark pink in the midsubstance with dark red lining surrounding the formerly demineralized brushite anchors (Figure 11). Under polarized light, there is evidence of collagen I (orange-red) and III (green) in all groups. Picrosirius red staining under polarized light allows for the distinction of collagen I and III. All three groups showed evidence of tissue penetration into the bone-mimicking anchor. Modular constructs had a greater degree of organic material penetration compared to the control and 400k group. One can especially observe a greater penetration at the bone side that exhibits the most compressive force (Figure 11). Collagen I was found across all three groups in the midsubstance and around the anchors. Additionally, tissue penetration into the anchor seen in H&E and picrosirius red seems to contain primarily type one collagen (Figure 11 and 12). Confirmed by the dark-pink color of the tissue within the formerly demineralized anchor and collagen I staining (figure 11 and 12). Collagen X fluorescence was also observed in all three groups, although it is less intense in the modular group, contrary to our hypothesis.

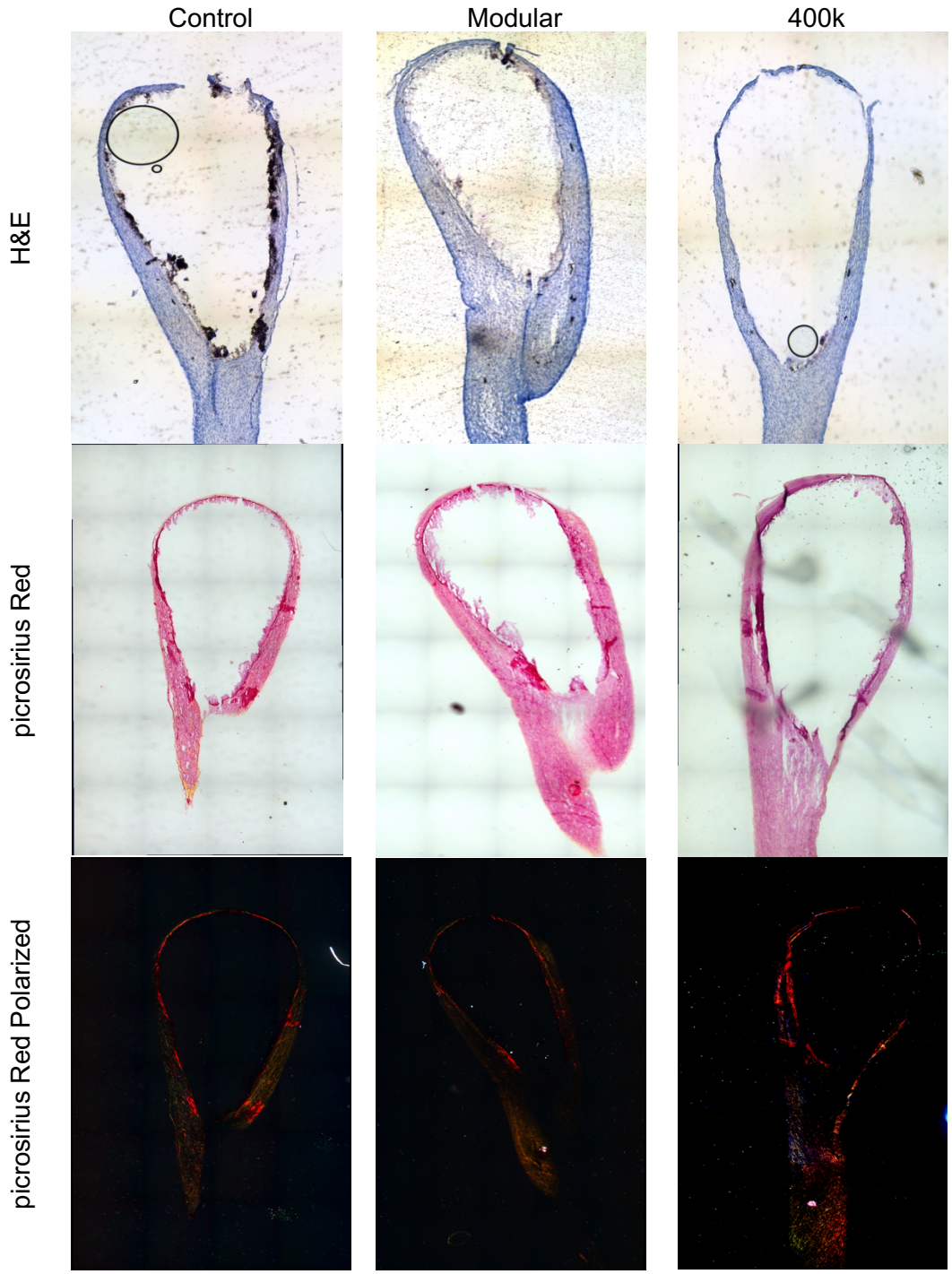

Figure 11. Evidence of tissue penetration in the formerly demineralized brushite anchor. Decalcified 14-day-old constructs were cryosectioned and stained with hematoxylin and eosin (H&E), picrosirius red brightfield, and Sirius red polarized light. Tissue infiltration into the demineralized brushite region was observed in all three groups, with more pronounced infiltration observed in modular constructs. Modular constructs also displayed a thick band of nuclei adjacent to the demineralized brushite region (C), which co-localized with a dense band of collagen (blue).

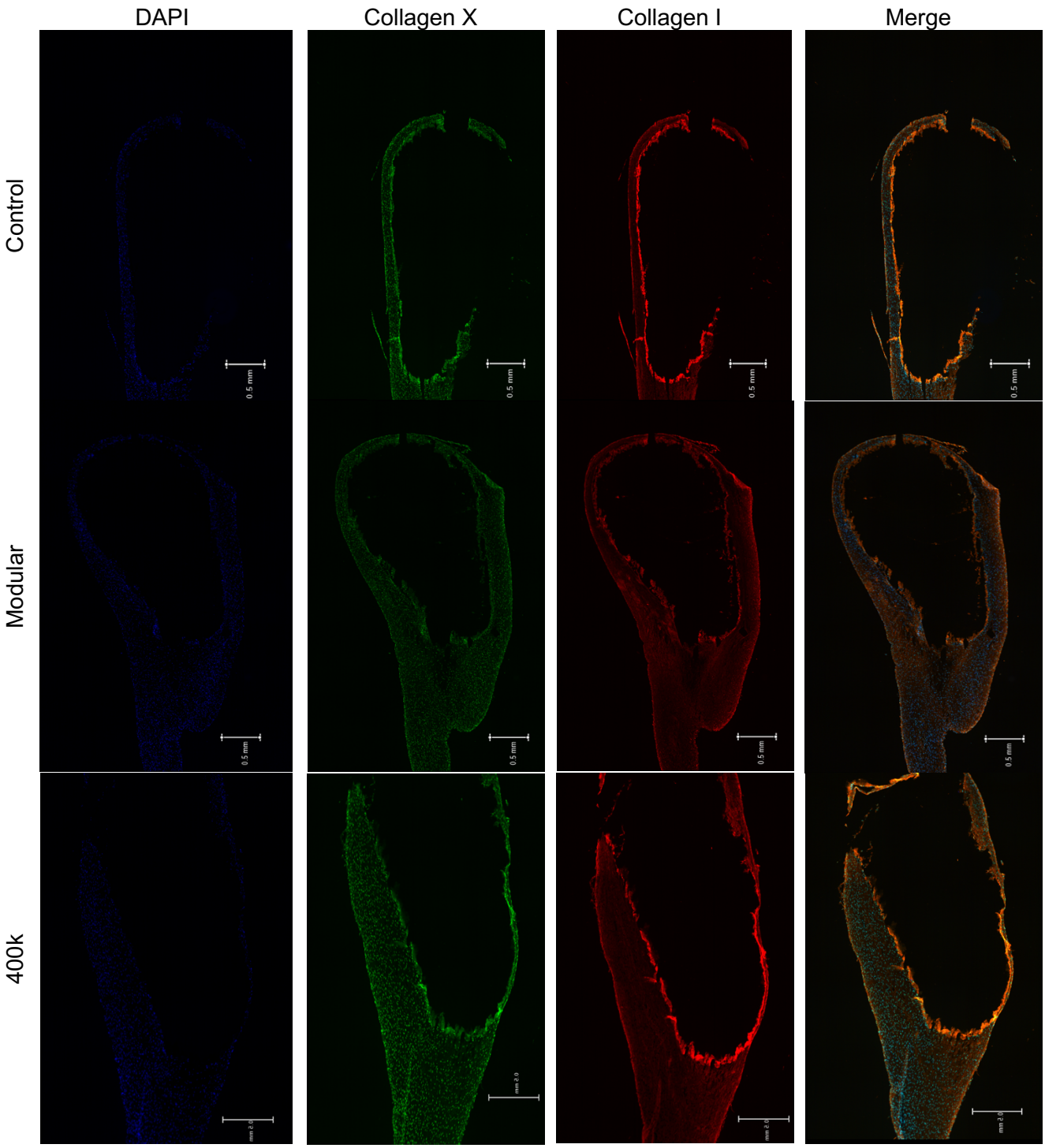
DAPI
Collagen X
Collagen I
Merge
Control
Modular
400k

Figure 12. Collagen I and Collagen X present adjacent to formerly demineralized anchor.
Immunohistochemistry of decalcified 14-day-old constructs. DAPI, Collagen I, Collagen X, and Merged Image. Collagen I was seen around the demineralized brushite anchor in all three groups. Tissue penetration consists of collagen I and X. Collagen X was less present in the modular group, between the tissue infiltration and where the brushite met.

Discussion

The aim of this study was to improve the interface between the ACL cells and bone to create bone-to-bone engineered ligaments and recapitulate the enthesis. To this end, this study used a modular approach to form 3-D engineered ligaments in an effort to improve the structural integrity at the interface. We formed enthesis tissue around two individual brushite anchors pre-seeded for five days before forming a linear construct. Creating extra tissue around the anchors allowed for a more continuous transition between the ligament and brushite anchor, unlike the normal, discontinuous constructs. The result of the extra tissue around the anchor was a 7-fold increase in failure in the midsubstance of the ligament. Despite the improved integration, the enthesis constructs did not show a significant increase in interface strength (measured by MTL) compared with either the control or 400k (cell control) groups. Even though the interface tended to be stronger, the localization of type X collagen was not improved, suggesting that the enthesis had not been recapitulated in these tissues. These data indicate that engineering more tissue around an anchor increases the strength of the ligament-bone interface without resulting in enthesis formation.

Interface strength was assessed via the maximal tensile load since previous studies in the lab demonstrated that construct failure mainly occurs at the interface between the soft tissue and the bone cement (Lee-Barthel et al., 2018). Our enthesis group (modular) did demonstrate an increase in the number of constructs that failed in the mid-substance of the soft tissue compared to the control and 400k groups. I was conservative in what I considered mid-substance failure. Failure at the middle of the ligament was considered a middle failure. By

contrast, I considered failure around the brushite anchors or where the mid-substance meets the enthesis tissue failure at the anchor. In reality, the modular constructs mostly failed between the enthesis tissue and mid-substance, which was still considered failure at the anchor. During complete anchor side failure, modular constructs tended to have more mineral content attached to the tissue than the control and 400k groups. In some cases, we also observed phenomena that mimicked an avulsion fracture where a small chunk of bone was removed at failure (data not shown), although this was a qualitative observation.

The collagen content of the modular constructs was significantly greater than the control and 400k groups. Although, this affect is normalized to the mass of the tissue to generate the collagen percentage, there was no significant difference between the groups. This might indicate that the five additional days in culture for the modular group, allowed the formation of proportionally more tissue mass around the anchor as a result of increased collagen.

In vivo, interfaces between tissues with different mechanical properties such as the bone-ligament or the tendon-bone complex, have variable mechanical properties to reduce strain concentrations. Tendons/ligaments have highly aligned, crimped collagen that makes the tissue anisotropic, thus making the tissue stronger in the longitudinal direction and weaker in the transverse direction (Lynch et al., 2003). This is achieved through various mechanisms including: 1) increasing collagen crosslinking and decreasing collagen alignment, 2) gradient in matrix composition and structure, 3) greater surface area of attachment, and 4) interdigitation of the transitional tissue with bone (Benjamin et al., 1995, 2000, 2006; Curwin et al., 1994; Shaw et al., 2008b).

In the engineered ligaments, we previously observed aligned collagen at the mid-substance of the ligament that becomes less aligned towards the boney end of the interface,

similar to what is observed in native tissue (Paxton et al., 2012). The decrease in collagen alignment allows for anchorage over a wide surface area giving the advantage of force transduction, reduction in stress concentrations, and protects bones by preventing fibers from bending acutely at hard tissue lines (Benjamin et al., 2006; Benjamin & Ralphs, 1998; Hems & Tillmann, 2000; Shaw & Benjamin, 2007). Modular constructs had greater tissue penetration (interdigitation) into the brushite anchor than the control and 400k groups. Tissue penetration into the formerly mineralized brushite anchor produces a kind of tidemark that would separate the mineralized fibrocartilage and unmineralized fibrocartilage *in vivo*. We believe there is a greater degree of tissue penetration at the opposing end of the brushite anchor due to more compressive forces as a result of contraction around the anchors. It is possible that this increased interdigitation decreased failure near the anchor.

To test whether there was a tidemark, immunohistochemistry staining of collagen I and X was performed. Collagen X is suggested to act as a growth plate between mineralized fibrocartilage and unmineralized fibrocartilage (Dyment, Hagiwara, et al., 2015; Fujioka et al., 1997; Galatz et al., 2007; G. Shen, 2005). We observed the presence of both collagen I and X throughout the engineered tissue including at sites of tissue penetration where the soft tissue and brushite anchor met. Previous *in vivo* studies conducted on neonatal mice suggest that collagen X appears at the tendon enthesis at day 14 of postnatal development. It is possible that our constructs have reached an equivalent maturity and therefore may be used in the future to elucidate physiological mechanisms of enthesis formation that may not be possible *in vivo*.

To make the extra tissue layer more like an enthesis, I would suggest three obvious starting points. First, different cell sources, such as human bone marrow stem cells (hBMSCs) or adipose-derived stem cells that have a greater potential to transdifferentiate into fibrocartilage

should be assessed. Second, growth factors such as BMPs, IGF, FGF, and HH agonists should be studied for their ability to promote enthesis formation. Third, the effect of cyclic tensile loading of the ligaments should be studied since loading is required for native enthesis formation.

The limitations of this study include a lack of quantification of enthesis-specific markers such as GAG, proteoglycans, and other ECM proteins. Cellular phenotypic studies assessing whether cells at the interface transdifferentiated into fibro-chondrocytes were also not conducted. Neither uniaxial nor compressive loads were added to the engineered ligaments. If loading is required to create the zonal differentiation of the enthesis this may mean that the enthesis would not form without external loading. Lastly, because to our model resembles an early sinew, further maturation may be necessary to localize collagen, proteoglycans, and other ECM proteins to the transition and form an enthesis.

Conclusion

Current tissue-engineered grafts for enthesis regeneration are immature and lack the essential component for transplantation: the transition site itself. This study used a modular approach to engineer bone-to-bone ligaments in an attempt to drive the formation of a functional enthesis. We demonstrated that adding extra tissue around the bone anchors increased interface resilience resulting in a 7-fold decrease in mechanical failure at the interface. The modular model also shows early signs of tissue penetration and integration between the bone and soft tissue. Given the potential application of this model, future studies that include using different cell sources in the enthesis anchors, growth factors and loading may help us better understand the formation of a functional soft tissue-bone interface.

Supplementary Figures:

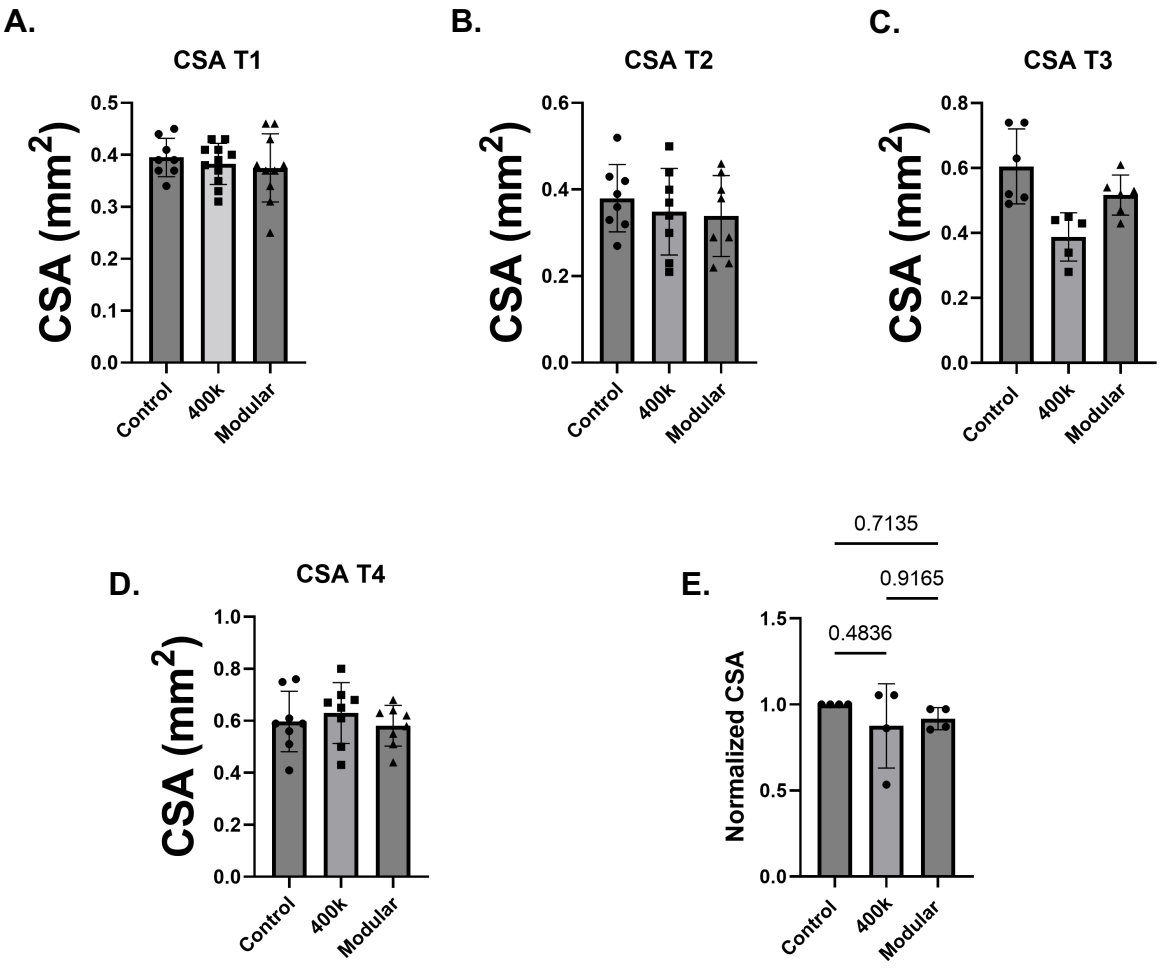

SF 1. No significant difference in cross-sectional area between groups. The cross-sectional area of control, 400k (cell-control), and modular groups across different biological replicates (A-D) and (E) a composite where the average of the technical replicates of each biological replicate are plotted together. T1 is representative of donor 1. T2 is the 2nd donor. T3 and T4 are the representation of hACL fibroblast cells from donor 3. A P-value of < 0.05 is to be considered statistically significant.

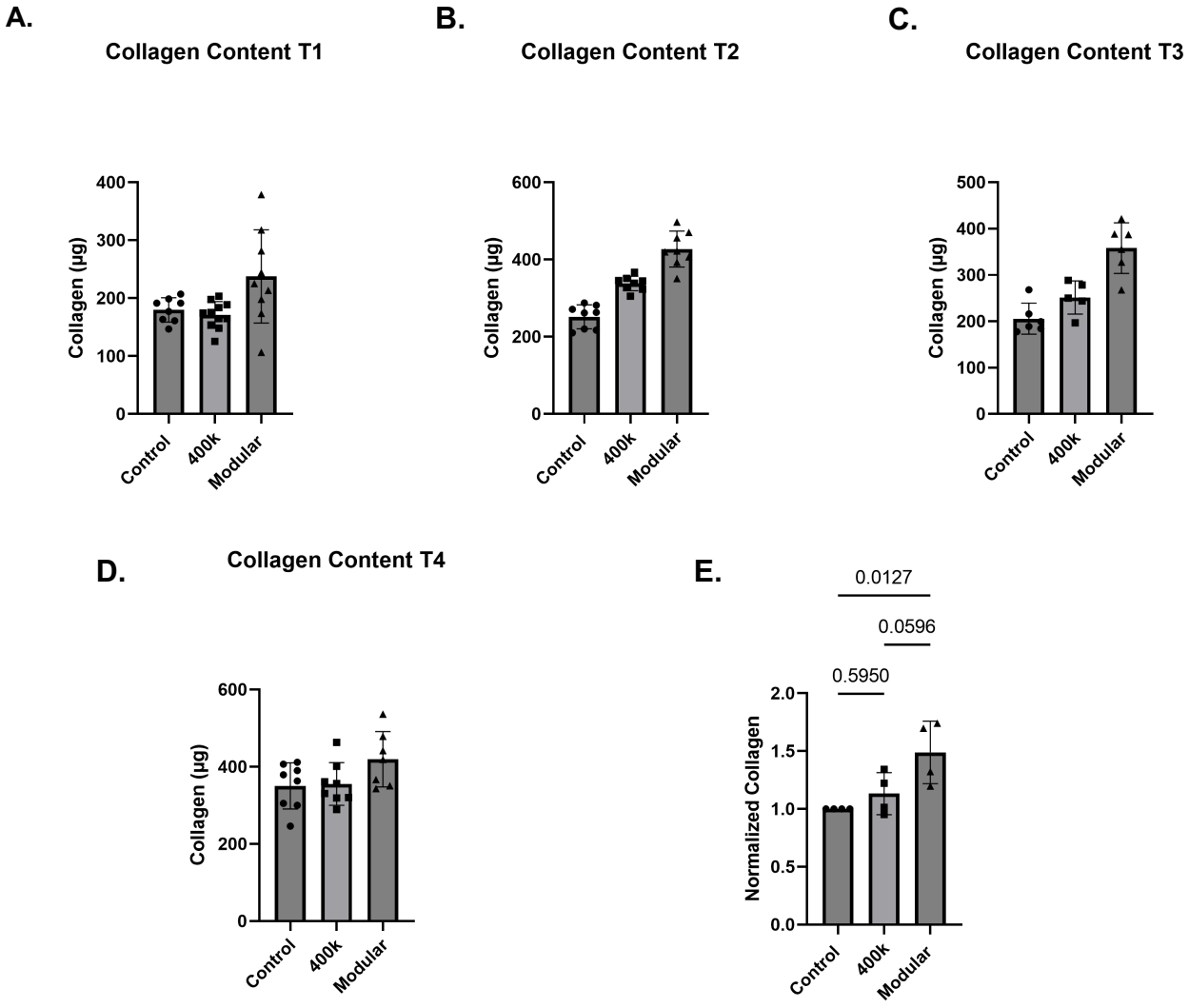

SF 2. Collagen content is higher in the modular group. The collagen content of control, 400k (cell-control), and modular groups across different biological replicates (A-D) and (E) a composite where the average of the technical replicates of each biological replicate are plotted together. T1 is representative of donor 1. T2 is the 2nd donor. T3 and T4 are the representation of hACL fibroblast cells from donor 3. A P-value of < 0.05 is to be considered statistically significant.

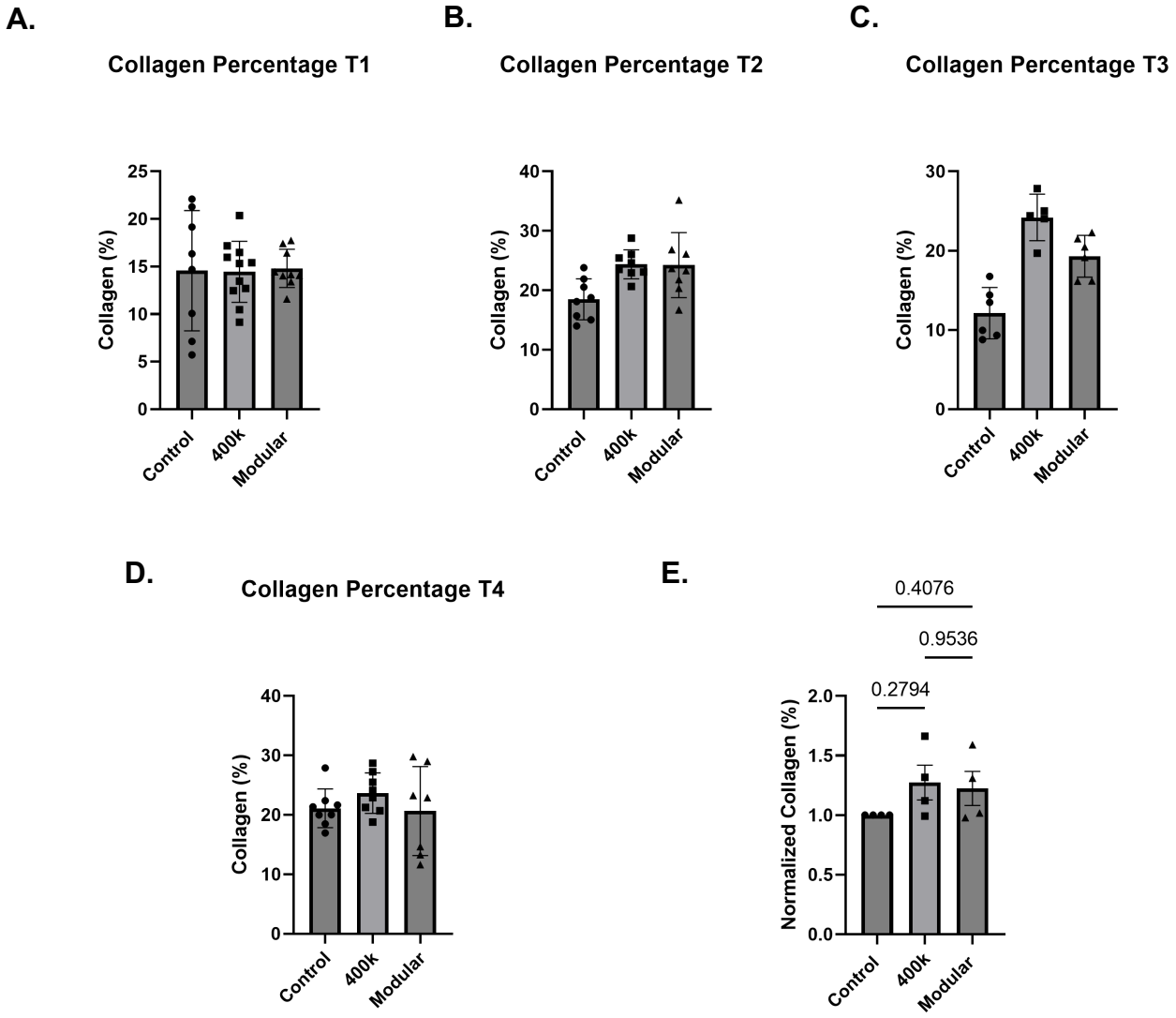

SF 3. The collagen fraction is not significantly different between groups. The collagen percentage of control, 400k (cell-control), and modular groups across different biological replicates (A-D) and (E) a composite where the average of the technical replicates of each biological replicate are plotted together. T1 is representative of donor 1. T2 is the 2nd donor. T3 and T4 are the representation of hACL fibroblast cells from donor 3. A P-value of < 0.05 is to be considered statistically significant.

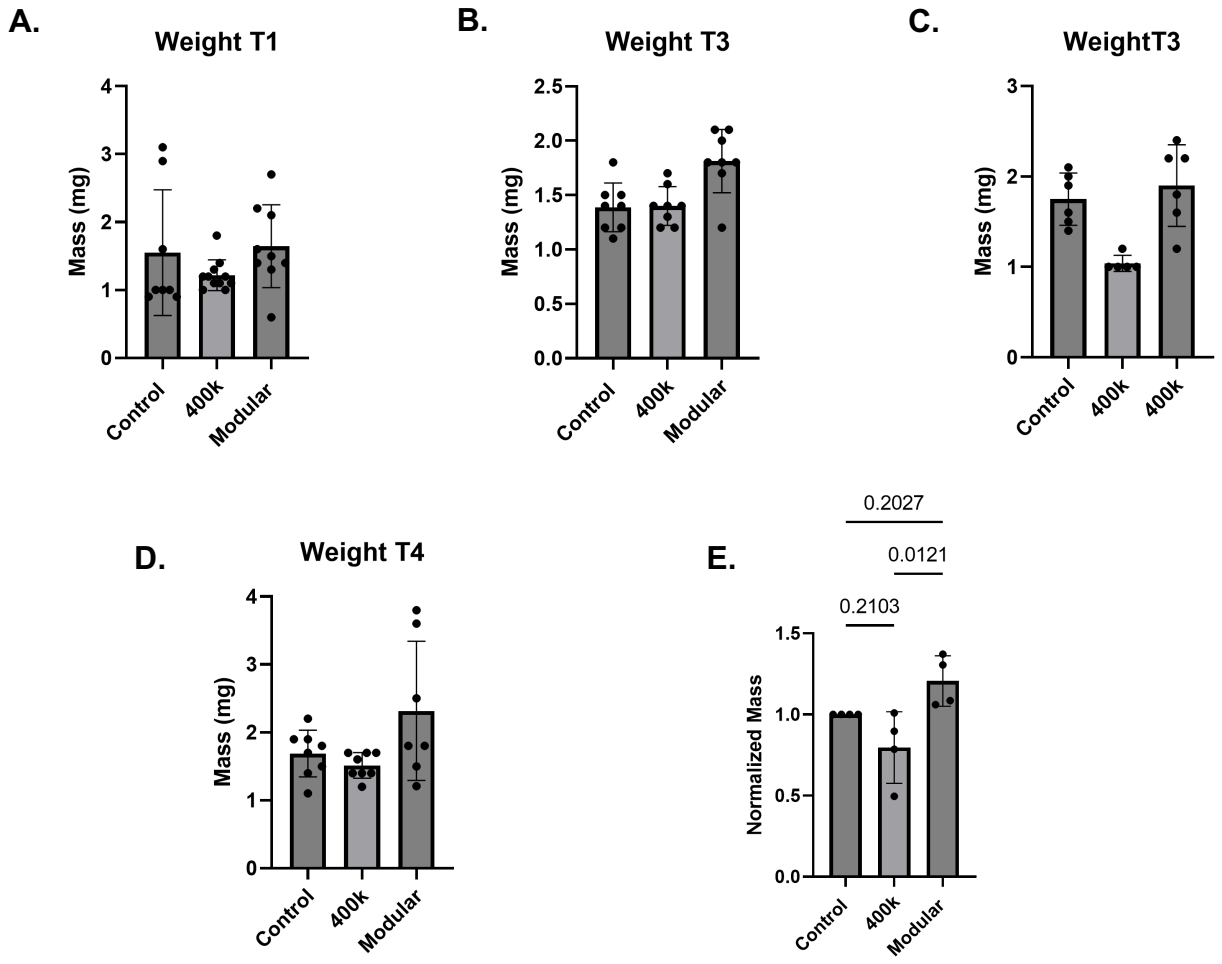

SF 4. No significant difference in collagen mass. Dry mass of control, 400k (cell-control), and modular groups across different biological replicates (A-D) and (E) a composite where the average of the technical replicates of each biological replicate are plotted together. T1 is representative of donor 1. T2 is the 2nd donor. T3 and T4 are the representation of hACL fibroblast cells from donor 3. A P-value of < 0.05 is to be considered statistically significant.

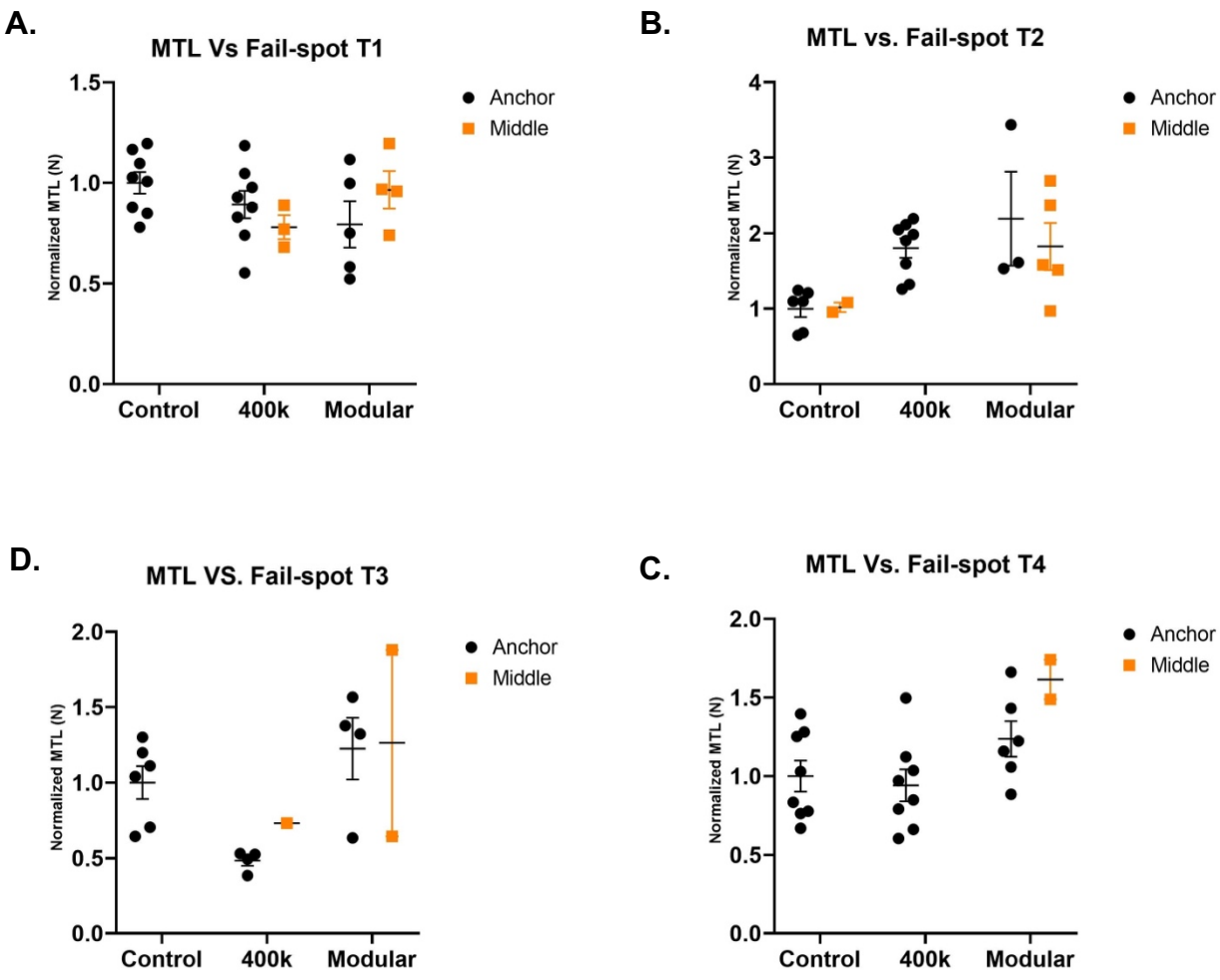

SF 5. Increased frequency of midsubtance is not due to increases in MTL. MTL vs fail-spot frequency of normalized data for control, 400k (cell-control), and modular groups across different biological replicates (A-D). T1 is representative of donor 1. T2 is the 2nd donor. T3 and T4 are the representation of hACL fibroblast cells from donor 3. A P-value of < 0.05 is to be considered statistically significant.

Works Cited

Almeida-Silveira, M. I., Lambertz, D., Peâ, C., & Goubel, F. (n.d.). *Changes in stiffness induced by hindlimb suspension in rat Achilles tendon*.

Asou, Y., Nifuji, A., Tsuji, K., Shinomiya, K., Olson, E. N., Koopman, P., Noda, M., & Surugadai Chiyodu-ku Tokyo, K. (2002). Departmrnt of Molc.cular Phurmacoloxy, Medical Re.ccwc/z Institute. In *Journal of Orthopaedic Research* (Vol. 20). www.elsevier.com/locatelortlires

Baker, B. M., Shah, R. P., Huang, A. H., & Mauck, R. L. (2011). Dynamic tensile loading improves the functional properties of mesenchymal stem cell-laden nanofiber-based fibrocartilage. *Tissue Engineering. Part A*, *17*(9–10), 1445–1455. https://doi.org/10.1089/TEN.TEA.2010.0535

Bangs, F., & Anderson, K. v. (n.d.). *Primary Cilia and Mammalian Hedgehog Signaling*. https://doi.org/10.1101/cshperspect.a028175

Banos, C. C., Thomas, A. H., & Kuo, C. K. (n.d.). *Collagen Fibrillogenesis in Tendon Development: Current Models and Regulation of Fibril Assembly*. https://doi.org/10.1002/bdrc.20130

Bedi, A., Kovacevic, D., Fox, A. J. S., Imhauser, C. W., Stasiak, M., Packer, J., Brophy, R. H., Deng, X. H., & Rodeo, S. A. (2010). Effect of early and delayed mechanical loading on tendon-to-bone healing after anterior cruciate ligament reconstruction. *The Journal of Bone and Joint Surgery. American Volume*, *92*(14), 2387–2401. https://doi.org/10.2106/JBJS.I.01270

Benjamin, M., & Mcgonagle, D. (n.d.). *Entheses: tendon and ligament attachment sites*. https://doi.org/10.1111/j.1600-0838.2009.00906.x

Benjamin, M., Moriggl, B., Brenner, E., Emery, P., Mcgonagle, D., & Redman, S. (2004). The "Enthesis Organ" Concept Why Enthesopathies May Not Present as Focal Insertional Disorders. *ARTHRITIS & RHEUMATISM*, *50*(10), 3306–3313. https://doi.org/10.1002/art.20566

Benjamin, M., & M Gonagle, D. (2001). The anatomical basis for disease localisation in seronegative spondyloarthropathy at entheses and related sites. In *J. Anat* (Vol. 199).

Benjamin, M., Qin, S., & Ralphs, J. R. (1995). Fibrocartilage associated with human tendons and their pulleys. In *J. Anat* (Vol. 187).

Benjamin, M., & Ralphs, J. R. (1998). Fibrocartilage in tendons and ligaments-an adaptation to compressive load. In *J. Anat*.

Benjamin, M., Rufai, A., & Ralphs, J. R. (2000). THE MECHANISM OF FORMATION OF BONY SPURS (ENTHESOPHYTES) IN THE ACHILLES TENDON. In *ARTHRITIS & RHEUMATISM* (Vol. 43, Issue 3).

Benjamin, M., Toumi, H., Ralphs, J. R., Bydder, G., Best, T. M., & Milz, S. (2006). Where tendons and ligaments meet bone: attachment sites ('entheses') in relation to exercise and/or mechanical load. In *J. Anat* (Vol. 208).

Blitz, E., Sharir, A., Akiyama, H., & Zelzer, E. (2013). Tendon-bone attachment unit is formed modularly by a distinct pool of Scx-and Sox9-positive progenitors. *Development (Cambridge)*, *140*(13), 2680–2690. https://doi.org/10.1242/dev.093906

Blitz, E., Viukov, S., Sharir, A., Shwartz, Y., Galloway, J. L., Pryce, B. A., Johnson, R. L., Tabin, C. J., Schweitzer, R., & Zelzer, E. (2009). Bone Ridge Patterning during Musculoskeletal Assembly Is Mediated through SCX Regulation of Bmp4 at the Tendon-

Skeleton Junction. *Developmental Cell*, *17*(6), 861–873. https://doi.org/10.1016/j.devcel.2009.10.010

Breidenbach, C.-F., Aschbacher-Smith, A., Butler, L., & Wylie, D. (2013a). A Role for Hedgehog Signaling in the Differentiation of the Insertion Site of the Patellar Tendon in the Mouse. *PLoS ONE*, *8*(6), 65411. https://doi.org/10.1371/journal.pone.0065411

Breidenbach, C.-F., Aschbacher-Smith, A., Butler, L., & Wylie, D. (2013b). A Role for Hedgehog Signaling in the Differentiation of the Insertion Site of the Patellar Tendon in the Mouse. *PLoS ONE*, *8*(6), 65411. https://doi.org/10.1371/journal.pone.0065411

Brown, M. E., & Puetzer, J. L. (2021). *ARTICLE IN PRESS Driving native-like zonal enthesis formation in engineered ligaments using mechanical boundary conditions and β-tricalcium phosphate*. https://doi.org/10.1016/j.actbio.2021.12.020

Butler, D. L., Juncosa, N., & Dressler, M. R. (2004). FUNCTIONAL EFFICACY OF TENDON REPAIR PROCESSES. *Annu. Rev. Biomed. Eng*, *6*, 303–332. https://doi.org/10.1146/annurev.bioeng.6.040803.140240

Calejo, I., Costa-Almeida, R., Gonçalves, A. I., Berdecka, D., Reis, R. L., & Gomes, M. E. (2018). Bi-directional modulation of cellular interactions in an in vitro co-culture model of tendon-to-bone interface. *Cell Proliferation*, *51*(6). https://doi.org/10.1111/CPR.12493

Carmel Vinestock, R., Felsenthal, N., Assaraf, E., Katz, E., Rubin, S., Krief, S., Dezorella, N., Levin-Zaidman, S., Thomopoulos, S., & Zelzer, E. (n.d.). *Neonatal enthesis healing involves non-inflammatory formation of acellular scar through 1 ECM secretion by resident cells 2*. https://doi.org/10.1101/2021.12.20.473454

Cillo, J. E., Gassner, R., Koepsel, R. R., & Buckley, M. J. (2000). Growth factor and cytokine gene expression in mechanically strained human osteoblast-like cells: implications for distraction osteogenesis. *Oral Surgery, Oral Medicine, Oral Pathology, Oral Radiology, and Endodontics*, *90*(2), 147–154. https://doi.org/10.1067/MOE.2000.107531

Clayton, S. W., Ban, G. I., Liu, C., & Serra, R. (2020). *Canonical and noncanonical TGF-β signaling regulate fibrous tissue differentiation in the axial skeleton*. https://doi.org/10.1038/s41598-020-78206-4

Curwin, S. L., Roy, R. R., & Vailas, A. C. (1994). Regional and age variations in growing tendon. *Journal of Morphology*, *221*(3), 309–320. https://doi.org/10.1002/JMOR.1052210306

Dagher, E., Hays, P. L., Kawamura, S., Godin, J., Deng, X. H., & Rodeo, S. A. (2009). Immobilization modulates macrophage accumulation in tendon-bone healing. *Clinical Orthopaedics and Related Research*, *467*(1), 281–287. https://doi.org/10.1007/S11999-008-0512-0

Dyment, N. A., Breidenbach, A. P., Schwartz, A. G., Russell, R. P., Aschbacher-Smith, L., Liu, H., Hagiwara, Y., Jiang, R., Thomopoulos, S., Butler, D. L., & Rowe, D. W. (2015). Gdf5 progenitors give rise to fibrocartilage cells that mineralize via hedgehog signaling to form the zonal enthesis. *Developmental Biology*, *405*(1), 96–107. https://doi.org/10.1016/j.ydbio.2015.06.020

Dyment, N. A., Hagiwara, Y., Jiang, X., Huang, J., Adams, D. J., & Rowe, D. W. (2015). Response of knee fibrocartilage to joint destabilization. *Osteoarthritis and Cartilage / OARS, Osteoarthritis Research Society*, *23*(6), 996. https://doi.org/10.1016/J.JOCA.2015.01.017

Eliasson, P., Andersson, T., Hammerman, M., & Aspenberg, P. (2013a). Primary gene response to mechanical loading in healing rat Achilles tendons. *J Appl Physiol*, *114*, 1519–1526. https://doi.org/10.1152/japplphysiol.01500.2012.-Loading

Eliasson, P., Andersson, T., Hammerman, M., & Aspenberg, P. (2013b). Primary gene response to mechanical loading in healing rat Achilles tendons. *Journal of Applied Physiology (Bethesda, Md. : 1985)*, *114*(11), 1519–1526. https://doi.org/10.1152/JAPPLPHYSIOL.01500.2012

Evanko, S. P., & Vogel, K. G. (1993). Proteoglycan Synthesis in Fetal Tendon Is Differentially Regulated by Cyclic Compression in Vitro. *Archives of Biochemistry and Biophysics*, *307*(1), 153–164. https://doi.org/10.1006/ABBI.1993.1574

Felsenthal, N., Rubin, S., Stern, T., Krief, S., Pal, D., Pryce, B. A., Schweitzer, R., & Zelzer, E. (2018). *Development of migrating tendon-bone attachments involves replacement of progenitor populations*. https://doi.org/10.1242/dev.165381

Friese, N., Gierschner, M. B., Schadzek, P., Roger, Y., & Hoffmann, A. (2020). Regeneration of Damaged Tendon-Bone Junctions (Entheses)—TAK1 as a Potential Node Factor. *International Journal of Molecular Sciences 2020, Vol. 21, Page 5177*, *21*(15), 5177. https://doi.org/10.3390/IJMS21155177

Fujioka, H., Wang, G. J., Mizuno, K., Balian, G., & Hurwitz, S. R. (1997). Changes in the expression of type-X collagen in the fibrocartilage of rat Achilles tendon attachment during development. *Journal of Orthopaedic Research : Official Publication of the Orthopaedic Research Society*, *15*(5), 675–681. https://doi.org/10.1002/JOR.1100150508

Galatz, L., Rothermich, S., VanderPloeg, K., Petersen, B., Sandell, L., & Thomopoulos, S. (2007). Development of the supraspinatus tendon-to-bone insertion: Localized expression of extracellular matrix and growth factor genes. *Journal of Orthopaedic Research*, *25*(12), 1621–1628. https://doi.org/10.1002/JOR.20441

Gardinier, E. S., Manal, K., Buchanan, T. S., & Snyder-Mackler, L. (2014). Clinically-relevant measures associated with altered contact forces in patients with anterior cruciate ligament deficiency. *Clinical Biomechanics (Bristol, Avon)*, *29*(5), 531–536. https://doi.org/10.1016/J.CLINBIOMECH.2014.03.011

Gaut, L., Robert, N., Delalande, A., Bonnin, M.-A., Pichon, C., & Duprez, D. (2016). *EGR1 Regulates Transcription Downstream of Mechanical Signals during Tendon Formation and Healing*. https://doi.org/10.1371/journal.pone.0166237

Golman, M., Abraham, A. C., Kurtaliaj, I., Marshall, B. P., Hu, Y. J., Schwartz, A. G., Edward Guo, X., Birman, V., Thurner, P. J., Genin, G. M., & Thomopoulos, S. (2021). Toughening mechanisms for the attachment of architectured materials: The mechanics of the tendon enthesis. *Science Advances*, *7*(48), 5584. https://doi.org/10.1126/SCIADV.ABI5584/SUPPL_FILE/SCIADV.ABI5584_MOVIES_S1_TO_S4.ZIP

Gorschewsky, O., Klakow, A., Riechert, K., Pitzl, M., & Becker, R. (2005). Clinical comparison of the Tutoplast allograft and autologous patellar tendon (bone-patellar tendon-bone) for the reconstruction of the anterior cruciate ligament: 2- and 6-year results. *The American Journal of Sports Medicine*, *33*(8), 1202–1209. https://doi.org/10.1177/0363546504271510

Han, X., Zhuang, Y., Zhang, Z., Guo, L., & Wang, W. (2016). *Regulatory Mechanisms of the Ihh/PTHrP Signaling Pathway in Fibrochondrocytes in Entheses of Pig Achilles Tendon*. https://doi.org/10.1155/2016/8235172

Harvey, A. K., Thompson, M. S., Cochlin, L. E., Raju, P. A., Cui, Z., Cornell, H. R., Hulley, P. A., & Brady, S. M. (2009). Functional Imaging of Tendon. *Annals of the BMVA*, *2009*(8), 1–11.

Heinemeier, K., Langberg, H., Olesen, J. L., & Kjaer, M. (2003). Role of TGF-β1 in relation to exercise-induced type I collagen synthesis in human tendinous tissue. *Journal of Applied Physiology*, *95*(6), 2390–2397. https://doi.org/10.1152/JAPPLPHYSIOL.00403.2003/ASSET/IMAGES/LARGE/DG1232721007.JPEG

Hems, T., & Tillmann, B. (2000). Tendon entheses of the human masticatory muscles. *Anatomy and Embryology*, *202*(3), 201–208. https://doi.org/10.1007/S004290000107

Herchenhan, A., Dietrich-Zagonel, F., Schjerling, P., Kjær, M., & Eliasson, P. (2020). Early Growth Response Genes Increases Rapidly After Mechanical Overloading and Unloading in Tendon Constructs. *Journal of Orthopaedic Research®*, *38*(1), 173–181. https://doi.org/10.1002/JOR.24513

Id, K. I., Tokunaga Id, T., Shukunami, C., Takimoto, A., Yoshimoto, Y., Yonemitsu, R., Karasugi, T., Mizuta, H., Hiraki, Y., & Miyamoto, T. (2020). *Role of Scx + /Sox9 + cells as potential progenitor cells for postnatal supraspinatus enthesis formation and healing after injury in mice*. https://doi.org/10.1371/journal.pone.0242286

Järvinen, T. A. H., Józsa, L., Kannus, P., Järvinen, T. L. N., Hurme, T., Kvist, M., Pelto-Huikko, M., Kalimo, H., & Järvinen, M. (2003). Mechanical loading regulates the expression of tenascin-C in the myotendinous junction and tendon but does not induce de novo synthesis in the skeletal muscle. *Journal of Cell Science*, *116*(Pt 5), 857–866. https://doi.org/10.1242/JCS.00303

Jiang, J., Nicoll, S. B., & Lu, H. H. (2005). Co-culture of osteoblasts and chondrocytes modulates cellular differentiation in vitro. *Biochemical and Biophysical Research Communications*, *338*(2), 762–770. https://doi.org/10.1016/J.BBRC.2005.10.025

Killian, M. L., & Thomopoulos, S. (n.d.). *Scleraxis is required for the development of a functional tendon enthesis; Scleraxis is required for the development of a functional tendon enthesis*. https://doi.org/10.1096/fj.14-258236

LaCroix, A. S., Duenwald-Kuehl, S. E., Lakes, R. S., & Vanderby, R. (2013). Relationship between tendon stiffness and failure: a metaanalysis. *Journal of Applied Physiology*, *115*(1), 43. https://doi.org/10.1152/JAPPLPHYSIOL.01449.2012

Larkin, L. M., Calve, S., Kostrominova, T. Y., & Arruda, E. M. (2006). Structure and Functional Evaluation of Tendon–Skeletal Muscle Constructs Engineered in Vitro. *Https://Home.Liebertpub.Com/Ten*, *12*(11), 3149–3158. https://doi.org/10.1089/TEN.2006.12.3149

Lee-Barthel, A., Lee, | C A, Vidal, | M A, Baar, | K, & Vidal, M. A. (2018). *Localized BMP-4 release improves the enthesis of engineered bone-to-bone ligaments*. https://doi.org/10.1002/tsm2.9

Leong, N. L., Kator, J. L., Clemens, T. L., James, A., Enamoto-Iwamoto, M., & Jiang, J. (2020). Tendon and Ligament Healing and Current Approaches to Tendon and Ligament Regeneration. *J Orthop Res*, *38*, 7–12. https://doi.org/10.1002/jor.24475

Li, Z., Yao, S.-J., Alini, M., & Stoddart, M. J. (n.d.). *Chondrogenesis of Human Bone Marrow Mesenchymal Stem Cells in Fibrin-Polyurethane Composites Is Modulated by Frequency and Amplitude of Dynamic Compression and Shear Stress*. www.liebertpub.com

Long, Z., Nakagawa, K., Wang, Z., Amadio, P. C., Zhao, | Chunfeng, & Gingery, A. (2021). *Age-related cellular and microstructural changes in the rotator cuff enthesis*. https://doi.org/10.1002/jor.25211

Lynch, H. A., Johannessen, W., Wu, J. P., Jawa, A., & Elliott, D. M. (2003). Effect of fiber orientation and strain rate on the nonlinear uniaxial tensile material properties of tendon. *Journal of Biomechanical Engineering*, *125*(5), 726–731. https://doi.org/10.1115/1.1614819

Maeda, E., Shelton, J. C., Bader, D. L., & Lee, D. A. (2009). Differential regulation of gene expression in isolated tendon fascicles exposed to cyclic tensile strain in vitro. *J Appl Physiol*, *106*, 506–512. https://doi.org/10.1152/japplphysiol.90981.2008.-Mechani

Maeda, T., Sakabe, T., Sunaga, A., Sakai, K., Rivera, A. L., Keene, D. R., Sasaki, T., Stavnezer, E., Iannotti, J., Schweitzer, R., Ilic, D., Baskaran, H., & Sakai, T. (2011). Conversion of mechanical force into TGF-β-mediated biochemical signals. *Current Biology : CB*, *21*(11), 933. https://doi.org/10.1016/J.CUB.2011.04.007

Magnusson, S. P., Langberg, H., & Kjaer, M. (2010). The pathogenesis of tendinopathy: balancing the response to loading. *Nature Reviews Rheumatology 2010 6:5*, *6*(5), 262–268. https://doi.org/10.1038/nrrheum.2010.43

Martinez-Lemus, L. A., Forte, G., Martino, F., Perestrelo, A. R., Vinarský, V., & Pagliari, S. (2018). *Cellular Mechanotransduction: From Tension to Function*. https://doi.org/10.3389/fphys.2018.00824

McCorry, M. C., Mansfield, M. M., Sha, X., Coppola, D. J., Lee, J. W., & Bonassar, L. J. (2017). A model system for developing a tissue engineered meniscal enthesis. *Acta Biomaterialia*, *56*, 110–117. https://doi.org/10.1016/J.ACTBIO.2016.10.040

Moffat, K. L., Sun, W.-H. S., Pena, P. E., Chahine, N. O., Doty, S. B., Ateshian, G. A., Hung, C. T., & Lu, H. H. (2008). *Characterization of the structure-function relationship at the ligament-to-bone interface*. www.pnas.org/cgi/content/full/

Mosher, C. Z., Spalazzi, J. P., & Lu, H. H. (2015). Stratified scaffold design for engineering composite tissues. *Methods (San Diego, Calif.)*, *84*, 99–102. https://doi.org/10.1016/J.YMETH.2015.03.029

Nowlin, J., Bismi, M. A., Delpech, B., Dumas, P., Zhou, Y., & Tan, G. Z. (2018). Engineering the hard–soft tissue interface with random-to-aligned nanofiber scaffolds. *Nanobiomedicine*, *5*, 184954351880353. https://doi.org/10.1177/1849543518803538

Paxton, J. Z., Grover, L. M., & Baar, K. (2010a). Engineering an in vitro model of a functional ligament from bone to bone. *Tissue Engineering. Part A*, *16*(11), 3515–3525. https://doi.org/10.1089/TEN.TEA.2010.0039

Paxton, J. Z., Grover, L. M., & Baar, K. (2010b). Engineering an in vitro model of a functional ligament from bone to bone. *Tissue Engineering - Part A*, *16*(11), 3515–3525. https://doi.org/10.1089/TEN.TEA.2010.0039/ASSET/IMAGES/LARGE/FIGURE7.JPEG

Paxton, J. Z., Hagerty, P., Andrick, J. J., & Baar, K. (2012). Optimizing an intermittent stretch paradigm using ERK1/2 phosphorylation results in increased collagen synthesis in engineered ligaments. *Tissue Engineering. Part A*, *18*(3–4), 277–284. https://doi.org/10.1089/TEN.TEA.2011.0336

Picrosirius Red Staining Protocol for Collagen. (n.d.). Retrieved September 4, 2022, from http://www.ihcworld.com/_protocols/special_stains/sirius_red.htm

Provot, S., & Schipani, E. (2005). Molecular mechanisms of endochondral bone development. In *Biochemical and Biophysical Research Communications* (Vol. 328, Issue 3, pp. 658–665). Academic Press Inc. https://doi.org/10.1016/j.bbrc.2004.11.068

Pryce, B. A., Watson, S. S., Murchison, N. D., Staverosky, J. A., Dünker, N., & Schweitzer, R. (2009). Recruitment and maintenance of tendon progenitors by TGFB signaling are essential for tendon formation. *Development*, *136*(8), 1351–1361. https://doi.org/10.1242/dev.027342

Puetzer, J. L., Ma, T., Sallent, I., Gelmi, A., & Stevens, M. M. (2021). Driving Hierarchical Collagen Fiber Formation for Functional Tendon, Ligament, and Meniscus Replacement. *Biomaterials*, *269*. https://doi.org/10.1016/j.biomaterials.2020.120527

Rossetti, L., Kuntz, L. A., Kunold, E., Schock, J., Müller, K. W., Grabmayr, H., Stolberg-Stolberg, J., Pfeiier, F., Sieber, S. A., Burgkart, R., & Bausch, A. R. (2017). *The microstructure and micromechanics of the tendon-bone insertion*. 27. https://doi.org/10.1038/NMAT4863

Saito, T., Nakamichi, R., Yoshida, A., Hiranaka, T., Okazaki, Y., Nezu, S., Matsuhashi, M., Shimamura, Y., Furumatsu, T., Nishida, K., & Ozaki, T. (2021). The effect of mechanical stress on enthesis homeostasis in a rat Achilles enthesis organ culture model. *Journal of Orthopaedic Research®*. https://doi.org/10.1002/JOR.25210

Salmon, L. J., Russell, V. J., Refshauge, K., Kader, D., Connolly, C., Linklater, J., & Pinczewski, L. A. (2006). Long-term outcome of endoscopic anterior cruciate ligament reconstruction with patellar tendon autograft: minimum 13-year review. *The American Journal of Sports Medicine*, *34*(5), 721–732. https://doi.org/10.1177/0363546505282626

Schwartz, A. G., Long, F., & Thomopoulos, S. (2015). *Enthesis fibrocartilage cells originate from a population of Hedgehog-responsive cells modulated by the loading environment*. https://doi.org/10.1242/dev.112714

Shaw, H. M., & Benjamin, M. (2007). Structure-function relationships of entheses in relation to mechanical load and exercise. *Scandinavian Journal of Medicine & Science in Sports*, *17*(4), 303–315. https://doi.org/10.1111/J.1600-0838.2007.00689.X

Shaw, H. M., Vázquez, O. T., Mcgonagle, D., Bydder, G., Santer, R. M., & Benjamin, M. (2008a). Development of the human Achilles tendon enthesis organ. *J. Anat*, *213*, 718–724. https://doi.org/10.1111/j.1469-7580.2008.00997.x

Shaw, H. M., Vázquez, O. T., Mcgonagle, D., Bydder, G., Santer, R. M., & Benjamin, M. (2008b). Development of the human Achilles tendon enthesis organ. *J. Anat*, *213*, 718–724. https://doi.org/10.1111/j.1469-7580.2008.00997.x

Shen, G. (2005). The role of type X collagen in facilitating and regulating endochondral ossification of articular cartilage. *Orthodontics & Craniofacial Research*, *8*(1), 11–17. https://doi.org/10.1111/J.1601-6343.2004.00308.X

Shen, H., Schwartz, A. G., Civitelli, R., & Thomopoulos, S. (2020). *Connexin 43 Is Necessary for Murine Tendon Enthesis Formation and Response to Loading*. https://doi.org/10.1002/jbmr.4018

Spalazzi, J. P., Dagher, E., Doty, S. B., Guo, X. E., Rodeo, S. A., & Lu, H. H. (2008). In vivo evaluation of a multiphased scaffold designed for orthopaedic interface tissue engineering and soft tissue-to-bone integration. *Journal of Biomedical Materials Research. Part A*, *86*(1), 1–12. https://doi.org/10.1002/JBM.A.32073

Spalazzi, J. P., Doty, S. B., Moffat, K. L., Levine, W. N., & Lu, H. H. (2006). Development of controlled matrix heterogeneity on a triphasic scaffold for orthopedic interface tissue engineering. *Tissue Engineering*, *12*(12), 3497–3508. https://doi.org/10.1089/TEN.2006.12.3497

Takimoto, A., Kawatsu, M., Yoshimoto, Y., Kawamoto, T., Seiryu, M., Takano-Yamamoto, T., Hiraki, Y., & Shukunami, C. (2015). *Scleraxis and osterix antagonistically regulate tensile force-responsive remodeling of the periodontal ligament and alveolar bone*. https://doi.org/10.1242/dev.116228

Thomopoulos, S., Das, R., Birman, V., Smith, L., Ku, K., Elson, E. L., Pryse, K. M., Marquez, J. P., & Genin, G. M. (2011). Fibrocartilage Tissue Engineering: The Role of the Stress Environment on Cell Morphology and Matrix Expression. *Https://Home.Liebertpub.Com/Tea*, *17*(7–8), 1039–1053. https://doi.org/10.1089/TEN.TEA.2009.0499

Thomopoulos, S., Kim, H.-M., Rothermich, S. Y., Biederstadt, C., Das, R., & Galatz, L. M. (2007). Decreased Muscle Loading Delays Maturation of the Tendon Enthesis during Postnatal Development. *J Orthop Res*, *25*, 1154–1163. https://doi.org/10.1002/jor.20418

Trensz, F., Haroun, S., Cloutier, A., Richter, M. v., & Grenier, G. (2010). A muscle resident cell population promotes fibrosis in hindlimb skeletal muscles of mdx mice through the Wnt canonical pathway. *American Journal of Physiology. Cell Physiology*, *299*(5). https://doi.org/10.1152/AJPCELL.00253.2010

Tsukamoto, N., Maeda, T., Miura, H., Jingushi, S., Hosokawa, A., Harimaya, K., Higaki, H., Kurata, K., & Iwamoto, Y. (2006). Repetitive tensile stress to rat caudal vertebrae inducing cartilage formation in the spinal ligaments: a possible role of mechanical stress in the development of ossification of the spinal ligaments. *Journal of Neurosurgery: Spine*, *5*(3), 234–242. https://doi.org/10.3171/SPI.2006.5.3.234

Wang, M., Vanhouten, J. N., Nasiri, A. R., Tommasini, S. M., & Broadus, A. E. (2014). Periosteal PTHrP regulates cortical bone modeling during linear growth in mice. *Journal of Anatomy*, *225*(1), 71. https://doi.org/10.1111/JOA.12184

Woessner, J. F. (1961). The determination of hydroxyproline in tissue and protein samples containing small proportions of this imino acid. *Archives of Biochemistry and Biophysics*, *93*(2), 440–447. https://doi.org/10.1016/0003-9861(61)90291-0

Xu, H. guang, Zhang, X. hai, Wang, H., Liu, P., Wang, L. ting, Zuo, C. jian, Tong, W. xue, & Zhang, X. ling. (2012). Intermittent Cyclic Mechanical Tension-Induced Calcification and downregulation of ankh gene expression of end plate chondrocytes. *Spine*, *37*(14), 1192–1197. https://doi.org/10.1097/BRS.0B013E318244D989